Journal of Medicinal Chemistry

Article

pubs.acs.org/jmc

Synthesis and Biological Evaluation (in Vitro and in Vivo) of Cyclic Arginine−Glycine−Aspartate (RGD) Peptidomimetic−Paclitaxel Conjugates Targeting Integrin $\alpha_V\beta_3$

Raffaele Colombo,[†] Michele Mingozzi,[†] Laura Belvisi,[†] Daniela Arosio,[‡] Umberto Piarulli,*[,§] Nives Carenini,[⊥] Paola Perego,[⊥] Nadia Zaffaroni,[⊥] Michelandrea De Cesare,[⊥] Vittoria Castiglioni,[∥] Eugenio Scanziani,[∥] and Cesare Gennari*[,†]

[†]Dipartimento di Chimica, Università degli Studi di Milano, Via Golgi 19, I-20133, Milan, Italy

[‡]CNR, Istituto di Scienze e Tecnologie Molecolari (ISTM), Via Golgi 19, I-20133, Milan, Italy

[§]Dipartimento di Scienza e Alta Tecnologia, Università degli Studi dell'Insubria, Via Valleggio 11, I-22100, Como, Italy

[⊥]Molecular Pharmacology Unit, Department of Experimental Oncology and Molecular Medicine, Fondazione IRCCS Istituto Nazionale Tumori, Via Amadeo 42, I-20133 Milan, Italy

[∥]Dipartimento di Scienze Veterinarie e Sanità Pubblica, Università degli Studi di Milano, Via Celoria 10, I-20133 Milan, Italy

Supporting Information

ABSTRACT: A small library of integrin ligand−paclitaxel conjugates **10**−**13** was synthesized with the aim of using the tumor-homing *cyclo*[DKP-RGD] peptidomimetics for site-directed delivery of the cytotoxic drug. All the paclitaxel−RGD constructs **10**−**13** inhibited biotinylated vitronectin binding to the purified $\alpha_V\beta_3$ integrin receptor at low nanomolar concentration and showed in vitro cytotoxic activity against a panel of human tumor cell lines similar to that of paclitaxel. Among the cell lines, the cisplatin-resistant IGROV-1/Pt1 cells expressed high levels of integrin $\alpha_V\beta_3$, making them attractive to be tested in in vivo models. *cyclo*[DKP-*f*3-RGD]-PTX **11** displayed sufficient stability in physiological solution and in both human and murine plasma to be a good candidate for in vivo testing. In tumor-targeting experiments against the IGROV-1/Pt1 human ovarian carcinoma xenotransplanted in nude mice, compound **11** exhibited a superior activity compared with paclitaxel, despite the lower (about half) molar dosage used.

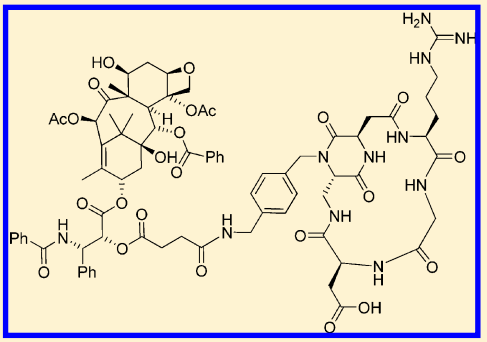

INTRODUCTION

Chemotherapy has been one of the main approaches for the treatment of cancer for more than half a century and is based on the administration of drugs that often interfere with fundamental cellular functions (e.g., DNA replication, cell division). The antitumor efficacy of anticancer drugs is thus limited by their nonspecific toxicity to normal cells, especially to rapidly growing cells such as blood, bone marrow, and mucous membrane cells, resulting in a low therapeutic index and serious side effects. The efficacy of chemotherapy is further limited by the occurrence or development of drug resistance: tumor cells can be regarded as a rapidly changing target because of their genetic instability, heterogeneity, and high rate of mutation, leading to selection and overgrowth of a drug-resistant tumor cell population.[1] In principle, the efficiency of the treatment can be improved by increasing the doses, but this approach commonly results in severe toxicity. Therefore, selective tumor targeting of chemotherapeutic agents represents a major goal, and various drug delivery systems have been recently developed,[2] including the use of liposomes, microspheres, micelles, polymers, protein−drug or antibody−drug conjugates, and prodrugs.[3] Considerable efforts are currently being made in this domain to such an extent that leaders of major pharmaceutical companies foresee that >60% of all existing drugs will be targeted in less than 2 decades.[4] In this field, an attractive avenue for selective tumor targeting are hybrid molecules designed to bind to specific overexpressed receptors on cancer cells.[5] Clearly, the success of this approach is heavily dependent on the rational selection of appropriate biological objectives.

Integrins are ideal pharmacological targets based on their key role in angiogenesis and tumor development and on their easy accessibility as cell surface receptors interacting with extracellular ligands.[6] They are bidirectional glycoprotein heterodimeric receptors that connect cells to the scaffolding proteins of the extracellular matrix, occurring in at least 24 pairs of 18 α and 8 β subunits and containing large extracellular domains and short cytoplasmic domains.[7] Integrins are also involved in tissue integrity and cell trafficking, growth, differentiation, proliferation, and migration.[8] As a consequence of their role in so many fundamental processes, integrin malfunction is connected

Received: July 20, 2012

dx.doi.org/10.1021/jm301058f | J. Med. Chem. XXXX, XXX, XXX−XXX

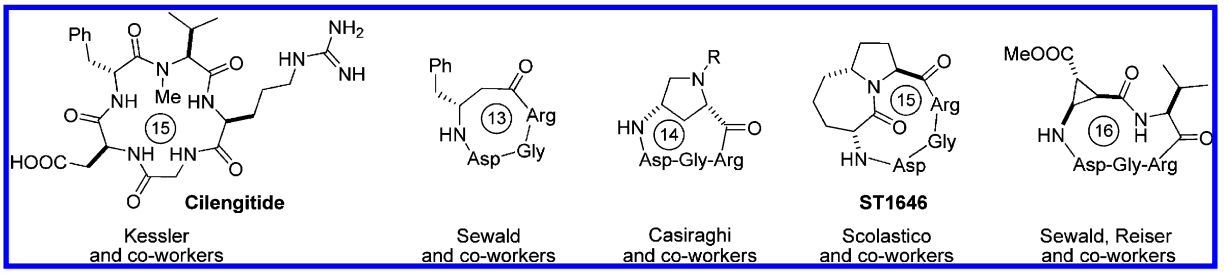

Figure 1. Potent $\alpha_V\beta_3$ integrin ligands.

to a large variety of diseases such as thrombosis, osteoporosis, inflammation, and cancer.[9] The tripeptide sequence arginine−glycine−aspartate (RGD) has been identified as the common motif used by several endogenous ligands to recognize and bind a group of integrins, including $\alpha_V\beta_3$, $\alpha_V\beta_5$, $\alpha_5\beta_1$, which are crucial in angiogenesis, tumor progression, and metastasis, and $\alpha_{IIb}\beta_3$, which is involved in platelet aggregation.[10]

A potent $\alpha_V\beta_3$ integrin ligand, *cyclo*[Arg-Gly-Asp-D-Phe-*N*(Me)-Val] (cilengitide) developed by Kessler and co-workers (Figure 1),[11,12] is currently in phase III clinical trials as an angiogenesis inhibitor for patients with glioblastoma multiforme.[13] The high activity and selectivity of this derivative have been attributed to an extended conformation of the RGD motif displaying a distance of about 9 Å between the C_β atoms of Asp and Arg.[12,14] These observations prompted many other research groups to investigate the use of conformationally constrained cyclic RGD peptidomimetics as active and selective integrin antagonists. A selection of these ligands, encompassing a wide variety of rigid scaffolds and featuring 13-, 14-, 15- and 16-membered rings, is shown in Figure 1.[15]

We have recently contributed to this field with a new class of cyclic RGD-peptidomimetics, containing bifunctional diketopiperazine (DKP) scaffolds and featuring 17-membered rings (Figure 2).[16] The cis-derivative *cyclo*[DKP-1-RGD] (**1**)

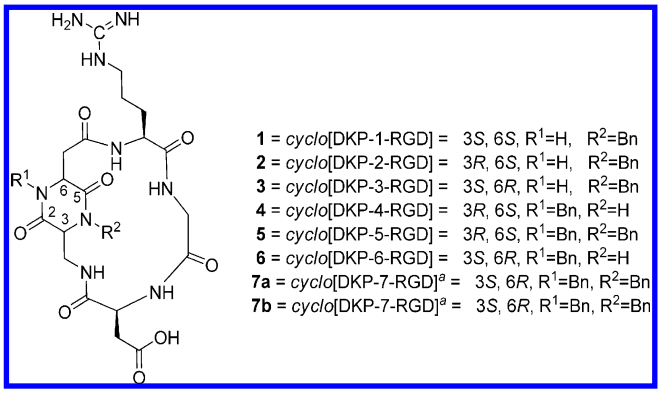

Figure 2. Library of *cyclo*[DKP-RGD] integrin ligands. [a]*N,N'*-Dibenzyl *cyclo*[DKP-7-RGD] was isolated as two different separable conformers (diastereomers, **7a** and **7b**) due to hindered rotation of one ring around the other, i.e., the DKP *N*-benzyl group cannot pass inside the macrolactam ring; see ref 16b.

inhibited biotinylated vitronectin binding to the purified $\alpha_V\beta_3$ receptor at a micromolar concentration (3.9 ± 0.4 μM), while trans-derivatives **2**−**7** ranged from submicromolar to subnanomolar concentrations (220−0.2 nM).

It is now emerging that antiangiogenic therapy alone is not sufficient to fight and eradicate tumors: recent preclinical findings of a paradoxical proangiogenic activity of RGD-mimetic agents (like cilengitide) at low concentrations have stimulated the debate on the use of antiangiogenetics as single drugs.[17] Since α_V integrins, which can be internalized by cells, are involved in tumor angiogenesis and are overexpressed on the surface of cancer cells, integrin ligands can be usefully employed as tumor-homing peptidomimetics for site-directed delivery of cytotoxic drugs.[18] During the past 15 years, a number of RGD-cytotoxic drug conjugates have been developed. In these approaches, a few cyclic RGD integrin ligands (e.g., RGD4C,[19] *cyclo*[(NMe)VRGDf-NH],[20] *cyclo*[RGDfK],[21,22] *cyclo*[CRGDC],[22] *cyclo*[RGDf-Aad],[23a] *cyclo*[RGDf-Amp][23a]) were conjugated to a cytotoxic drug (e.g., doxorubicin,[19,21] doxsaliform,[20] camptothecin,[23a,b] cisplatin[22]) through different linkers, such as amides,[19,22,23a] oximes,[20,23a] maleimides,[21] carbamates,[23b] and idrazones.[23a] Notably, Chen and co-workers prepared the RGD ligand−paclitaxel conjugate **8** (Figure 3), which was covalently assembled by joining the

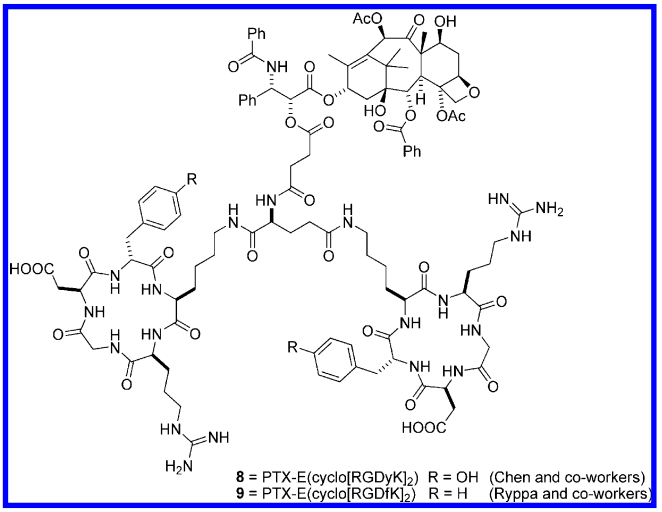

Figure 3. Dimeric RGD ligand−paclitaxel conjugates.

microtubule-stabilizing anticancer agent to the dimeric RGD peptide E[*cyclo*(RGDyK)]$_2$ via a cleavable succinyl ester linker, and evaluated its antitumor activity on the metastatic breast cancer cell line MDA-MB-435.[24] In mice, conjugate **8** showed a moderately improved antitumor effect over paclitaxel, but no tumor regression could be observed. The stability of the succinyl linker was not assessed and a premature release of paclitaxel can be suspected.

A very similar conjugate (i.e., compound **9** reported in Figure 3) was extensively evaluated in a recent study by Ryppa and co-workers on an ovarian carcinoma xenograft model (OVCAR-3).[25] Although the construct provided promising results in vitro, unfortunately it did not show any antitumor effect in vivo. The stability of conjugate **9** in a glucose phosphate buffer

dx.doi.org/10.1021/jm301058f | J. Med. Chem. XXXX, XXX, XXX−XXX

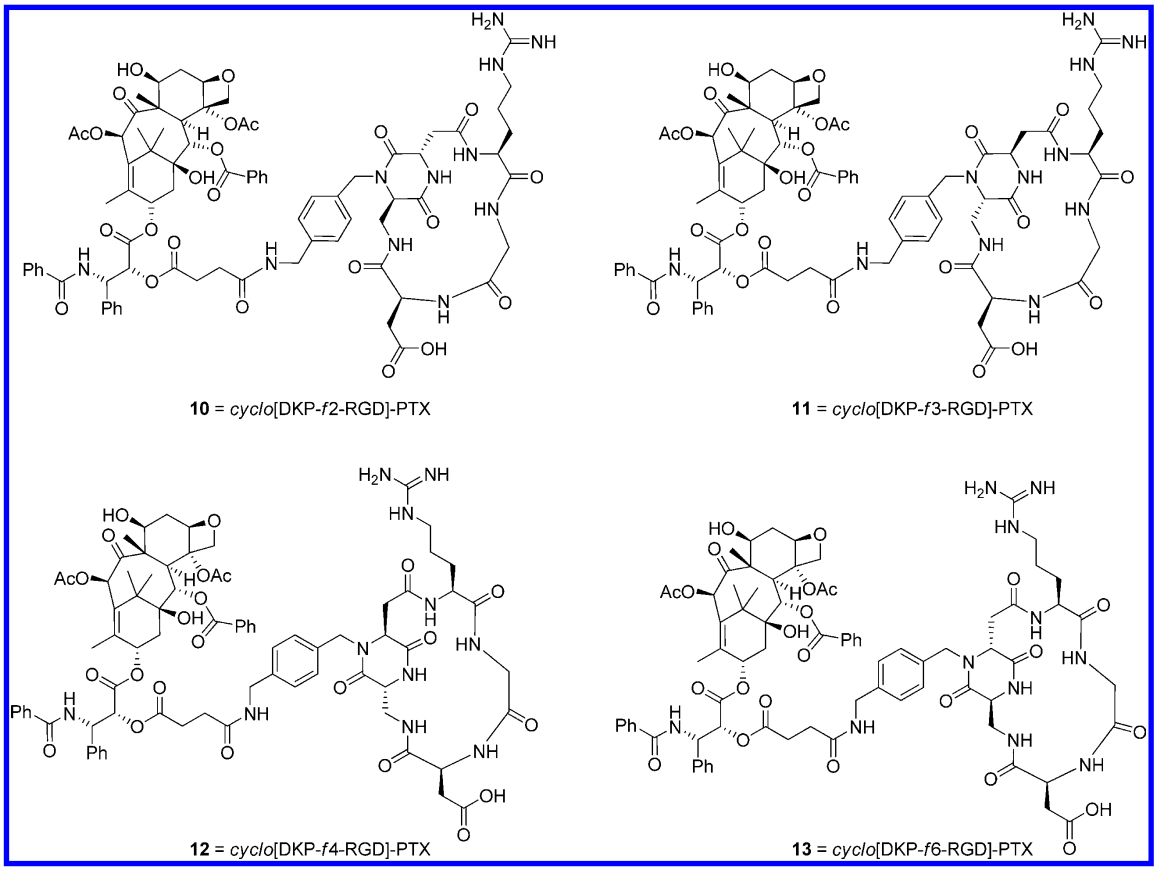

Figure 4. Structures of *cyclo*[DKP-RGD]−paclitaxel conjugates **10**−**13**.

solution at pH 7 was studied over 24 h, yielding a half-life of only ∼2 h at 37 °C. Half-life in the bloodstream is expected to be much shorter, and the inefficacy of this conjugate was attributed to hydrolysis of the ester bond at the 2′ position of paclitaxel, which causes premature release of the cytotoxic agent and loss of the tumor-homing effect.

Herein, we present a full account of our investigations reporting (i) the synthesis of new *cyclo*[DKP-RGD] integrin ligands, bearing a free amine group suitable for conjugation to a cytotoxic drug, (ii) the conjugation of these ligands to paclitaxel via a succinyl linker to give *cyclo*[DKP-RGD]−paclitaxel conjugates **10**−**13** (Figure 4), (iii) the stability of a *cyclo*[DKP-RGD]−paclitaxel construct in a physiological solution and in both human and murine plasma, which turned out to be far better than the case reported above,[25] (iv) the ability of the *cyclo*[DKP-RGD]−paclitaxel conjugates to compete with biotinylated vitronectin for binding to the purified $\alpha_V\beta_3$ and $\alpha_V\beta_5$ receptors, (v) in vitro cytotoxic activity of the *cyclo*[DKP-RGD]−paclitaxel conjugates in a panel of human cancer cell lines, (vi) in vivo tumor-targeting efficacy against the IGROV-1/Pt1 human ovarian carcinoma xenotransplanted in nude mice, (vii) the effects of tumor treatment, analyzed using immunohistochemistry.

RESULTS AND DISCUSSION

Synthesis. In order to prepare cyclic RGD peptidomimetics covalently linked to paclitaxel (compounds **10**−**13**, Figure 4), four functionalized (*f*) trans diketopiperazines (i.e., DKP-*f*2, DKP-*f*3, DKP-*f*4, DKP-*f*6) were synthesized, varying the position of the *p*-aminomethylbenzyl *N*-substituent (N-1 or N-4) and the absolute stereochemistry at C-3 and C-6 (Schemes 1−3). These DKPs were used for the synthesis of *cyclo*[DKP-RGD] integrin ligands (Scheme 4), which were conjugated to 2′-succinyl paclitaxel (Scheme 5).

Scheme 1. Synthesis of Aldehyde 14[a]

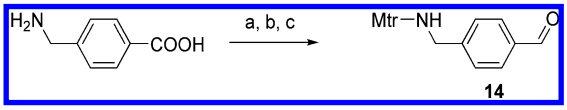

[a]Reagents and conditions: (a) $LiAlH_4$, THF, 8 h, reflux, 70%; (b) Mtr-Cl, *i*-Pr_2NEt, THF, 6 h, room temp, 85%; (c) MnO_2, THF, overnight, room temp, quant

For the preparation of the functionalized trans diketopiperazines DKP-*f*2, DKP-*f*3, DKP-*f*4, and DKP-*f*6, we selected a linker bearing both an aldehyde (for successive reductive alkylation) and an amino group (for the final conjugation to paclitaxel). Thus, linker **14** was synthesized in three steps from 4-aminomethylbenzoic acid via $LiAlH_4$ reduction, primary amine protection as 4-methoxy-2,3,6-trimethylbenzenesulfonamide (Mtr), and a benzylic alcohol oxidation using activated MnO_2 (Scheme 1). The Mtr protecting group was chosen because of its stability and orthogonality with the methyl, benzyl, allyl, *t*-Bu, Boc, and Cbz protecting groups.

Trans scaffolds DKP-*f*2, DKP-*f*3 (Scheme 2) and DKP-*f*4, DKP-*f*6 (Scheme 3) were synthesized starting from commercially available (*R*)- or (*S*)-aspartic acid and (*R*)- or (*S*)-serine. Two different synthetic strategies were developed depending on the nitrogen substitution. In particular, the synthesis of DKP-*f*2 and DKP-*f*3 (bearing the linker on DKP nitrogen N-4, former serine nitrogen) was realized making use of a serine

dx.doi.org/10.1021/jm301058f | J. Med. Chem. XXXX, XXX, XXX−XXX

Scheme 2. Synthesis of DKP-*f*2 and DKP-*f*3[a]

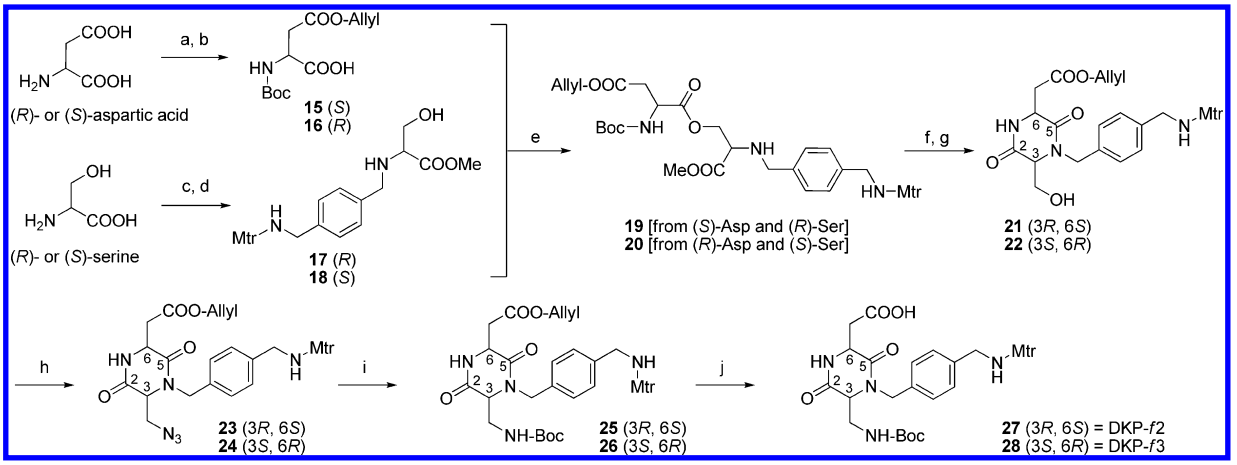

[a]Reagents and conditions: (a) allyl alcohol, AcCl; (b) Boc_2O, TEA, dioxane, water, 95% over two steps; (c) MeOH, AcCl, quant; (d) aldehyde **14**, $NaBH(OAc)_3$, THF, 3 h, room temp, quant; (e) HATU, HOAT, *i*-Pr_2NEt, DMF, 3 h, 0 °C to room temp, 86%; (f) TFA/DCM 1:2, 3 h, 0 °C to room temp; (g) *i*-Pr_2NEt, *i*-PrOH, 6 h, room temp, 93% over two steps; (h) HN_3·Tol, DIAD, Ph_3P, DCM/Tol 1:2, 7 h, −20 °C, 86%; (i) Me_3P, BOC-ON, THF, 6 h, −20 °C to room temp, 88%; (j) pyrrolidine, PPh_3, $[Pd(PPh_3)_4]$, DCM, 4 h, room temp, quant. Yields reported are the average of six experiments, including different reaction batches with the two enantiomeric products.

Scheme 3. Synthesis of DKP-*f*4 and DKP-*f*6[a]

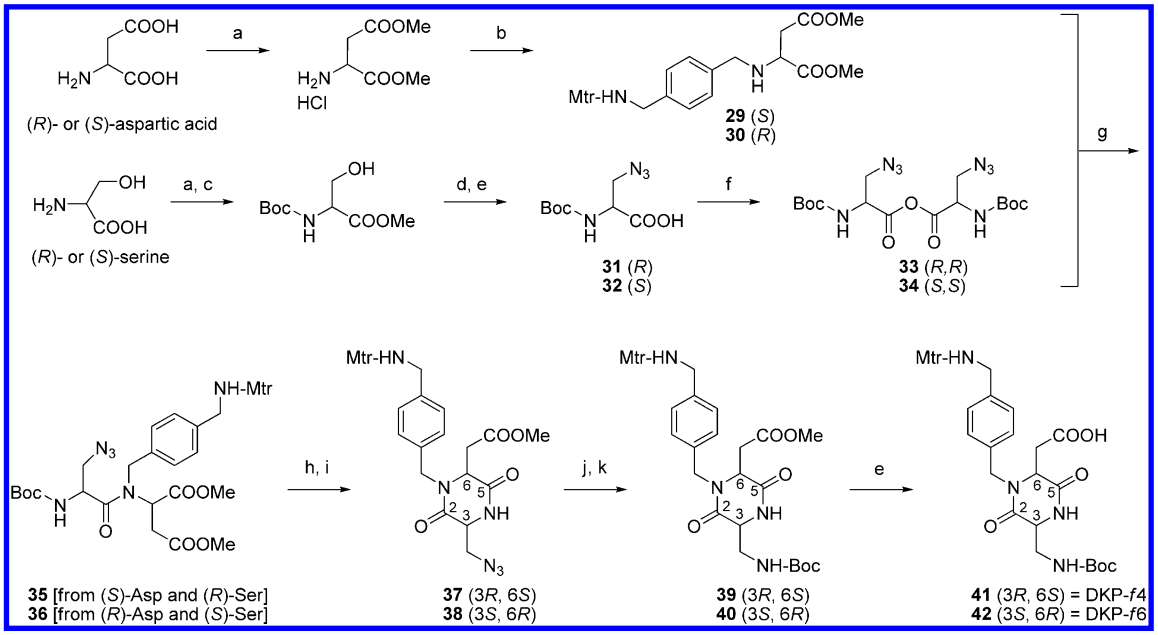

[a]Reagents and conditions: (a) MeOH, AcCl, quant; (b) aldehyde **14**, $NaBH_3(CN)$, MeOH, 4 h, room temp, 66%; (c) Boc_2O, TEA, dioxane−water, 95%; (d) HN_3·Tol, DIAD, Ph_3P, THF, 7 h, −20 °C, 78%; (e) LiOH, H_2O/THF 1:1, 1 h, 0 °C, quant; (f) DCC, DCM, 1 h, room temp, quant; (g) DCM, overnight, room temp, 40%; (h) TFA, Et_3SiH, DCM, 3 h, room temp, quant; (i) *i*-Pr_2NEt, *i*-PrOH, 6 h, room temp, 92%; (j) H_2, 10% Pd/C, THF, 4 h, room temp, quant; (k) Boc_2O, *i*-Pr_2NEt, DCM, 6 h, room temp, 96%. Yields reported are the average of six experiments, including different reaction batches with the two enantiomeric products.

ligation strategy,[26] as described in Scheme 2. (*R*)- and (*S*)-Aspartic acid were initially protected as allyl ester on the side chain and as *N*-Boc to give the enantiomeric derivatives (*S*)-**15** and (*R*)-**16**. (*R*)- and (*S*)-Serine were protected as methyl ester and reductively alkylated with aldehyde **14** and sodium triacetoxyborohydride to afford the enantiomeric compounds (*R*)-**17** and (*S*)-**18**. Direct coupling (HATU, *i*-Pr_2NEt) of protected aspartic acid (*S*)-**15** with functionalized serine (*R*)-**17**, or of the enantiomers (*R*)-**16** with (*S*)-**18**, led to the isopeptides (*S*,*R*)-**19** and (*R*,*S*)-**20** in high yield (86%) rather than forming the expected dipeptides. The *O*,*N*-acyl migration[26] was then triggered by cleavage of the Boc protecting group and treatment with a base (*i*-Pr_2NEt) in a protic solvent (*i*-PrOH), which also promoted the simultaneous cyclization to the trans diketopiperazines **21** and **22** (93% overall yield). The hydroxyl group of **21** and **22** was converted into azides **23** and **24** via a Mitsunobu reaction in good yield (86%), using HN_3·Tol in a toluene/dichloromethane solution. Finally, a one-pot Staudinger reduction−Boc protection followed by allyl deprotection yielded the trans scaffolds DKP-*f*2 (**27**, 3*R*,6*S*) and DKP-*f*3 (**28**, 3*S*,6*R*) in 88% yield. This synthetic route involves a high overall yield (60%) and only a few

dx.doi.org/10.1021/jm301058f | J. Med. Chem. XXXX, XXX, XXX−XXX

Scheme 4. Synthesis of Functionalized *cyclo*[DKP-RGD] Integrin Ligands 63−66[a]

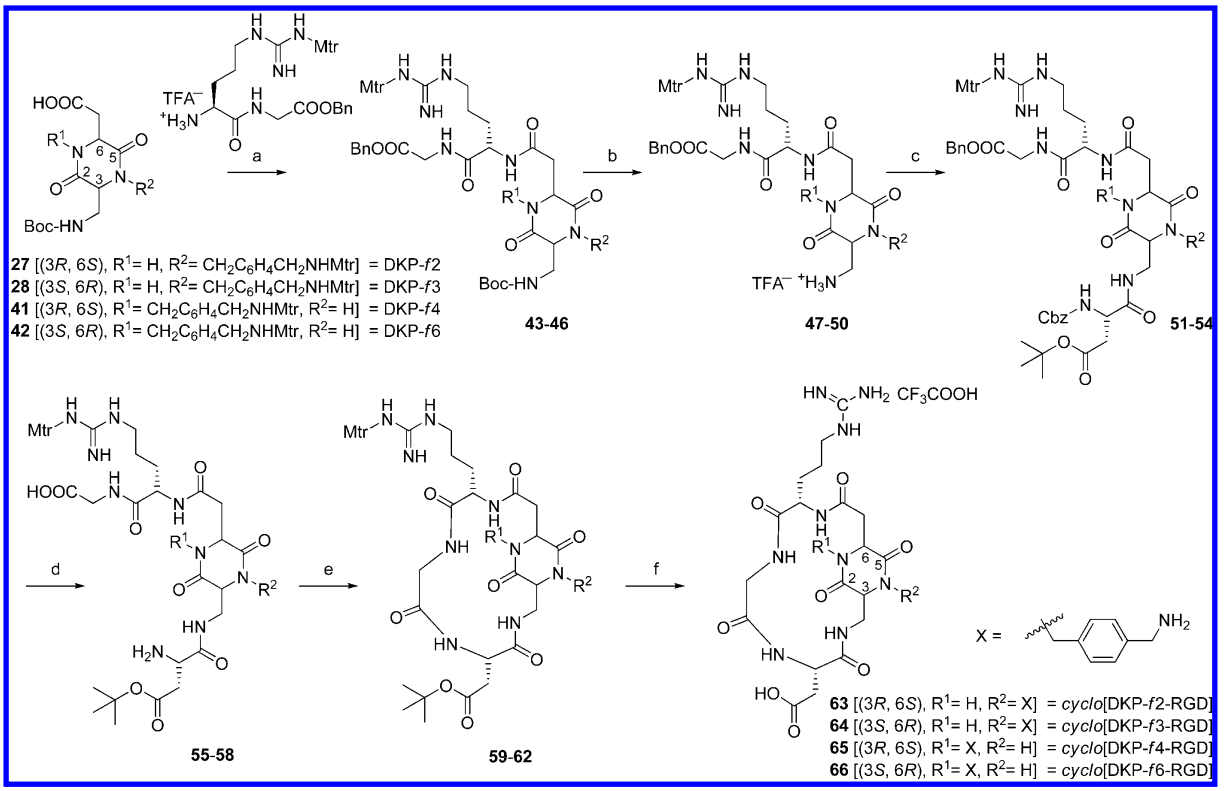

[a]Reagents and conditions: (a) HATU, HOAT, *i*-Pr_2NEt, DMF, overnight, room temp, 83−85%; (b) TFA/DCM 1:2, 3 h, room temp, quant; (c) Cbz-Asp(O-*t*-Bu)-OH, HATU, HOAT, *i*-Pr_2NEt, DMF, overnight, room temp, 86−88%; (d) H_2, 10% Pd/C, THF/H_2O 1:1, overnight, room temp, quant; (e) HATU, HOAT, *i*-Pr_2NEt, 1.4 mM in DMF, overnight, room temp, 60−81%; (f) TFA/TMSBr/thioanisol/EDT/phenol 70:14:10:5:1, 2 h, room temp, 70−85%.

chromatographic purifications, which allows easy preparation on a multigram scale.

For the synthesis of trans scaffolds DKP-*f*4 and DKP-*f*6 (Scheme 3), (*R*)- and (*S*)-aspartic acid were protected as dimethyl ester and reductively alkylated with aldehyde **14** to obtain the enantiomeric derivatives (*S*)-**29** and (*R*)-**30**. The hydroxyl group of (*R*)- or (*S*)-Boc-Ser-OMe was first transformed into the corresponding azide under Mitsunobu conditions in 78% yield, and then the methyl ester was saponified. The resulting enantiomeric acids (*R*)-**31** and (*S*)-**32**, stable only for a few hours, were immediately self-condensed with DCC in DCM to give the symmetric anhydrides (*R*,*R*)-**33** and (*S*,*S*)-**34**, which were isolated by filtering off the *N*,*N*′-dicyclohexylurea (DCU) and immediately reacted with the functionalized aspartic acid dimethyl ester (*S*)-**29** or (*R*)-**30** to obtain the enantiomeric dipeptides (*S*,*R*)-**35** and (*R*,*S*)-**36** in moderate yield (40%). Yield optimization was pursued by extensively varying the reaction conditions (equivalents, solvents, temperature, time), but all the attempts were not successful and markedly differed from the analogous reaction run on *N*-benzylaspartic acid dimethyl ester (i.e., **29** or **30** missing the Mtr-NH-CH_2- side chain) where the yield was uniformly higher (80%).[16b] All other coupling reagents tested (HATU, PyBrOP, DPPA, etc.) were ineffective for this reaction. Although no coupling product of the dehydroalanine derivative was ever detected, the *β*-elimination possibly caused by excess *i*-Pr_2NEt in the HATU, PyBrOP, and DPPA tentative couplings might be an additional reason for this failure, combined with the poor reactivity of the sterically hindered secondary amine of the aspartic derivative.

After Boc deprotection, the six-membered cyclization occurred spontaneously with 4 equiv of *i*-Pr_2NEt in *i*-PrOH to give diketopiperazines (3*R*,6*S*)-**37** and (3*S*,6*R*)-**38** in 92% yield. Trans scaffolds DKP-*f*4 (**41**, 3*R*,6*S*) and DKP-*f*6 (**42**, 3*S*,6*R*) were finally obtained by catalytic hydrogenation of the azide, Boc protection of the primary amine, and hydrolysis of the methyl ester (96% overall yield).

Trans diketopiperazines DKP-*f*2, DKP-*f*3, DKP-*f*4, and DKP-*f*6 were used as scaffolds for the synthesis of functionalized *cyclo*[DKP-RGD] integrin ligands **63−66**, following a solution-phase strategy (Scheme 4). Dipeptide Boc-Arg(Mtr)-Gly-OBn, prepared on a multigram scale following our reported procedure,[16b] was Boc-deprotected and coupled to the chosen diketopiperazine scaffold to give compounds **43−46** in good yields (83−85%). The Boc protecting group of compounds **43−46** was then removed, and the resulting free amines **47−50** were coupled to Cbz-Asp(O-*t*-Bu)-OH to obtain the linear Cbz-Asp(O-*t*-Bu)-DKP-Arg(Mtr)-Gly-OBn peptidomimetics **51−54** in high yields (86−88%). After carboxybenzyl and benzyl groups simultaneous deprotection by catalytic hydrogenolysis to give **55−58** quantitatively, the synthesis of protected *cyclo*(DKP-RGD) **59−62** was accomplished in good yield (60−81%) by 17-membered macrolactamization in a highly diluted DMF solution (1.4 mM) utilizing HATU, HAOT, and *i*-Pr_2NEt (4:4:6 equiv). The final step was the nontrivial removal of the side chain protecting groups.

The O-*t*-Bu and the Mtr on the arginine were easily deprotected, while the Mtr on the benzylic amine was very stable. Several cleavage cocktails were screened and the more classic ones[27] ["reagent K" (TFA/phenol/water/TIPS, 88/5/

dx.doi.org/10.1021/jm301058f | J. Med. Chem. XXXX, XXX, XXX−XXX

Scheme 5. Synthesis of *cyclo*[DKP-RGD]-PTX Conjugates 10−13[a]

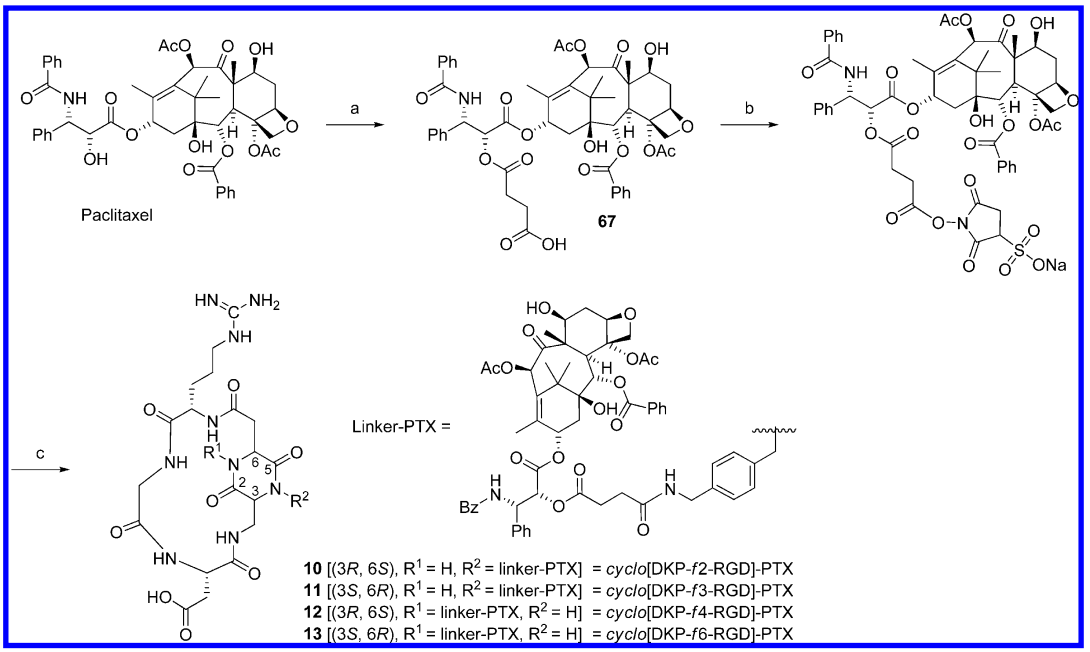

[a]Reagents and conditions: (a) succinic anhydride, py, DCM, overnight, 0 °C to room temp, 94%; (b) *N*-hydroxysulfosuccinimide sodium salt, DIC, DMF, overnight, room temp; (c) *cyclo*(DKP-RGD) **63**, **64**, **65**, or **66**, CH_3CN, aq phosphate buffer, pH 7.3, 10 h at 0 °C, then 8 h at room temp, 60−70%.

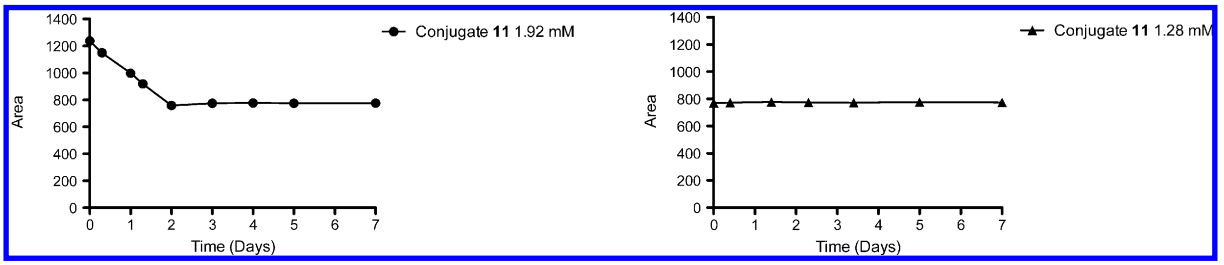

Figure 5. Solubility and stability of *cyclo*[DKP-*f*3-RGD]-PTX **11** in a physiological solution. Shown is the quantitative HPLC determination of solubility and stability of compound **11** in a physiological solution (0.9% NaCl in H_2O)/Cremophor EL/ethanol (90:5:5 v/v). A 1.92 mM clear solution of **11** turned out to be oversaturated and slowly flocculated to reach a concentration of 1.28 mM in 2 days (left diagram). The 1.28 mM solution did not undergo any precipitation or decomposition over 7 days (right diagram).

5/2), "reagent R" (TFA/thioanisole/EDT/anisole, 90/5/3/2), and "reagent P+" (TFA/phenol/methanesulfonic acid, 95/2.5/2.5)] failed, giving the monoprotected compound as the main product (the Mtr on the amine was still present), with a low yield (5−20%) of the desired totally deprotected product, even after 48 h. Finally, with the use of TFA/TMSBr/thioanisole/EDT/phenol (70/14/10/5/1) cleavage cocktail at room temperature for 2 h, fully deprotected compounds **63**−**66** were obtained in 70−85% isolated yield.

Thus, we were ready to conjugate paclitaxel to our ligands. The 2′-hydroxyl function of paclitaxel was derivatized with succinic anhydride, following a reported procedure.[28] The resulting paclitaxel hemisuccinate ester **67**[28] was activated using diisopropylcarbodiimide (DIC) and *N*-hydroxysulfosuccinimide sodium salt (sulfo-NHS), followed by coupling with *cyclo*[DKP-RGD] ligands **63**−**66** (Scheme 5).

The conjugation yield was strongly pH-dependent: at pH <7.0 the reaction did not proceed, whereas at pH >7.5 the hydrolysis of the sulfo-NHS ester substantially competed with the primary amine reaction. The synthesis of conjugates **10**−**13** was finally achieved in good yield (60−70%) by adding a 0.1 M aqueous NaOH solution when required throughout the reaction, for maintaining the pH at 7.3.

Solubility and Stability in a Physiological Solution. The solubility of conjugate *cyclo*[DKP-*f*3-RGD]-PTX **11** was investigated in a physiological solution (0.9% NaCl in H_2O)/Cremophor EL/ethanol (90:5:5 v/v) by quantitative HPLC. A 1.92 mM clear solution turned out to be oversaturated and slowly flocculated to reach a concentration of 1.28 mM in 2 days (Figure 5, left diagram). The precipitate was the conjugate **11** itself, with a purity of >99.5%. Compound **11** (1.28 μmol), dissolved in 0.1 mL of Cremophor EL/ethanol (1:1 v/v) and diluted with 0.9 mL of physiological solution, was perfectly stable for 1 week with a purity of >99.5%. The 1.28 mM solution did not undergo any precipitation or decomposition (Figure 5, right diagram).

Plasma Stability Assays. Paclitaxel conjugate **11** (1.28 μmol) was dissolved in DMSO (128 μL) and then diluted with pH 7.5 phosphate buffer (PBS) to give a 200 μM stock solution. Murine plasma was spiked with the stock solution to obtain a final 10 μM concentration and incubated at 37 °C. At time points varying from 1 to 330 min, aliquots of 50 μL were

dx.doi.org/10.1021/jm301058f | J. Med. Chem. XXXX, XXX, XXX−XXX

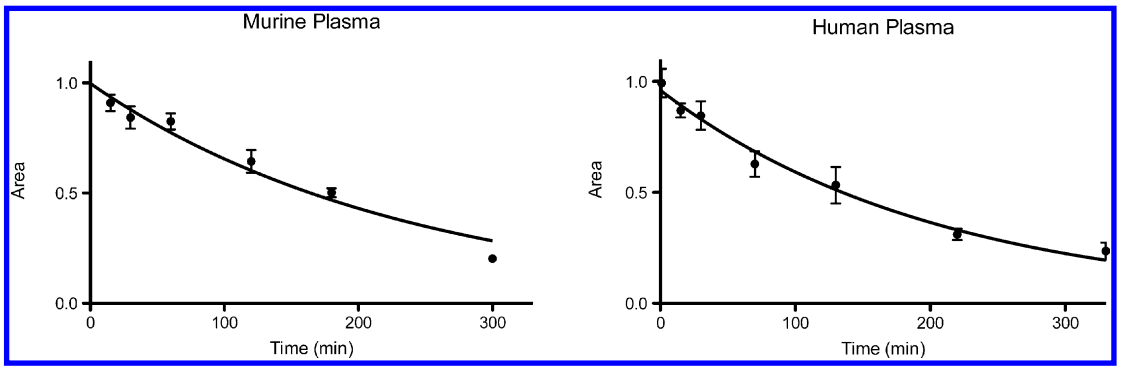

Figure 6. Stability of *cyclo*[DKP-*f*3-RGD]-PTX **11** in murine and human plasma. Shown is the quantitative HPLC determination of stability of compound **11** (10 μM) in murine plasma (left diagram) and in human plasma (right diagram) at 37 °C.

Table 1. Inhibition of Biotinylated Vitronectin Binding to $\alpha_v\beta_3$ and $\alpha_v\beta_5$ Receptors

		IC_{50} (nM)[a]	
compd	structure	$\alpha_v\beta_3$	$\alpha_v\beta_5$
10	*cyclo*[DKP-*f*2-RGD]-PTX[b]	8.5 ± 0.8	518 ± 10
11	*cyclo*[DKP-*f*3-RGD]-PTX[b]	5.2 ± 2.3	219 ± 124
12	*cyclo*[DKP-*f*4-RGD]-PTX[b]	0.9 ± 0.6	76 ± 32
13	*cyclo*[DKP-*f*6-RGD]-PTX[b]	1.1 ± 0.1	22 ± 3
64	*cyclo*[DKP-*f*3-RGD][c]	26.4 ± 3.7	>5 × 10^3
68	*cyclo*[DKP-*f*3-RGD]−hemisuccinamide[d]	4.1 ± 0.6	75 ± 1
2	*cyclo*[DKP-2-RGD][e]	3.2 ± 2.7	114 ± 99
3	*cyclo*[DKP-3-RGD][e]	4.5 ± 1.1	149 ± 25
4	*cyclo*[DKP-4-RGD][e]	7.6 ± 4.3	216 ± 5
6	*cyclo*[DKP-6-RGD][e]	2.1 ± 0.6	79 ± 3
cyclo[RGDfV][f]	*cyclo*[RGDfV]	3.2 ± 1.3	7.5 ± 4.8
ST1646[f]	ST1646[g]	1.0 ± 0.5	1.4 ± 0.8

[a]IC_{50} values were calculated as the concentration of compound required for 50% inhibition of biotinylated vitronectin binding as estimated by GraphPad Prism software. All values are the arithmetic mean ± SD of triplicate determinations. [b]See Figure 4. [c]See Scheme 4. [d]Compound **68** (see Figure 7) was synthesized as described in the Supporting Information. [e]See Figure 2. [f]Reference compound. [g]See Figure 1.

taken and quenched with 200 μL of ice-cold acetonitrile (containing verapamil as internal standard; see the Experimental Section for details). Samples were centrifuged at 3000 rpm for 20 min, and the supernatant was analyzed by RP-HPLC, UV−MS/MS. The data were fitted using a signal phase exponential decay and the calculated half-life was 165 ± 2 min (Figure 6, left diagram). The same procedure was adopted for a pooled human plasma stability assay, and in this case the calculated half-life was 143 ± 3 min (Figure 6, right diagram). Free paclitaxel accumulated during the assays as a result of hydrolysis of the succinyl ester bond at the PTX-2′ position. These results were very encouraging and showed that *cyclo*[DKP-*f*3-RGD]-PTX **11** is sufficiently stable to undergo animal testing with murine models. In fact, similar RGD ligands showed significant (maximum) tumor uptakes in mice after 10,[29] 20,[30] 30,[31] and 60 min.[32]

Summarizing, we have investigated the stability of compound **11** to hydrolysis both in a physiological solution and in murine and human plasma. As a matter of fact, *cyclo*[DKP-*f*3-RGD]-PTX **11** turned out to be far more stable than PTX-E[*cyclo*(RGDfK)]$_2$ **9**[25] (see Figure 3 and the relevant discussion in the Introduction). The rather high stability of **11** can possibly be attributed to a more lipophilic structure, where the ester linkage is less accessible in the protic medium than in Ryppa's compound **9**.

Integrin Receptors Competitive Binding Assays. *cyclo*[DKP-RGD]-PTX conjugates **10**−**13** were examined in vitro for their ability to inhibit biotinylated vitronectin binding to the purified $\alpha_v\beta_3$ and $\alpha_v\beta_5$ receptors and compared to their unfunctionalized analogues **2**, **3**, **4**, and **6** to the unconjugated ligands **64** and **68** and to the reference compounds *cyclo*[RGDfV][33] and ST1646.[34] The results are collected in Table 1. Screening assays were performed incubating the immobilized integrin receptors with various concentrations (10^{-12}−10^{-5} M) of the RGD ligands in the presence of biotinylated vitronectin (1 μg/mL) and measuring the concentration of bound vitronectin in the presence of the competitive ligands. Low nanomolar values were obtained with all the paclitaxel−RGD constructs (**10**−**13**), comparable to the unfunctionalized ligands (**2**, **3**, **4**, and **6**). These data reassured us that the enormous increase of steric hindrance in the *cyclo*[DKP-RGD]-PTX conjugates, due to presence of the linker bearing paclitaxel through the succinate tether, did not influence the high affinity for integrin receptors $\alpha_v\beta_3$ and $\alpha_v\beta_5$. Notably, for inhibition of vitronectin binding to the $\alpha_v\beta_3$ receptor, unconjugated ligand **64** required a 5-fold higher concentration than both its unfunctionalized and conjugated analogues (compounds **3** and **11**, respectively). This reduced affinity may result from perturbation of the electrostatic clamp (i.e., the binding interactions of the carboxylate and guanidinium groups with the charged regions of the receptor),[14] induced by the free amine present in **64**.

Derivatization of the amine with succinic anhydride gave the hemisuccinamide **68** and restored the high binding affinity for

dx.doi.org/10.1021/jm301058f | J. Med. Chem. XXXX, XXX, XXX−XXX

the $\alpha_v\beta_3$ receptor. Interestingly, unlike reference compounds *cyclo*(RGDfV) and ST1646, the *cyclo*[DKP-RGD] peptidomimetics were about 20- to 200-fold more selective for the $\alpha_v\beta_3$ integrin with respect to the $\alpha_v\beta_5$ in this kind of assay.

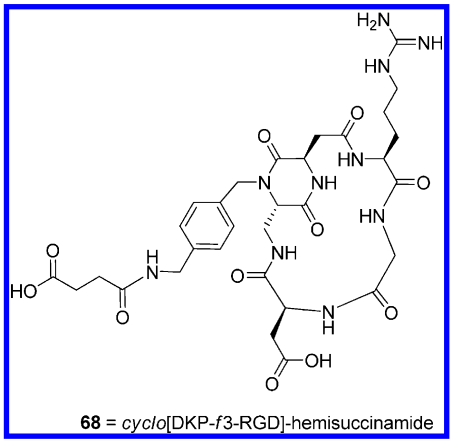

Figure 7. *cyclo*[DKP-*f*3-RGD]−hemisuccinamide.

Sensitivity of Tumor Cell Lines Treated with *cyclo*[DKP-RGD]-PTX Conjugates 10−13. *cyclo*[DKP-RGD]-PTX conjugates **10−13** were tested in vitro for their cytotoxic activity in comparison with paclitaxel, against a panel of human tumor cell lines. The cell sensitivity assays (Table 2) clearly indicated that the functionalized *cyclo*[DKP-*f*3-RGD] integrin ligand **64** was not cytotoxic, while the *cyclo*[DKP-RGD]-PTX conjugates displayed a cytotoxic activity similar to that of paclitaxel (same order of magnitude). These data imply that free paclitaxel is released at some stage, possibly after the conjugates have been internalized into the cells, because it is well-known that the free 2′-OH group is necessary for paclitaxel to exert its cytotoxic and microtubule-stabilizing activities.[35] Compounds **10−13**, **64**, and paclitaxel were also tested in vitro on normal HDFC fibroblasts. When cells started to proliferate and were exposed to different concentrations of these compounds (range of concentrations tested, 64−1000 nM), a marginal inhibition of cell growth was observed. The effect was not concentration-dependent, suggesting that the compounds were not cytotoxic but were at best cytostatic in these cells. The data reported in Table 2 did not identify undoubtedly a lead compound for evaluation of antitumor activity with in vivo models. Therefore, we chose *cyclo*[DKP-*f*3-RGD]-PTX **11** as our lead conjugate mainly because of its straightforward synthetic accessibility on a multigram scale.

Flow cytometry was used to detect the expression of $\alpha_V\beta_3$ and $\alpha_V\beta_5$ integrins on the surface of the different cancer cell lines (Table 3). Among these, the cisplatin-resistant IGROV-1/Pt1 cells expressed very high levels of integrin $\alpha_V\beta_3$, making them attractive to be tested in murine models with *cyclo*[DKP-RGD]-PTX construct **11** (vide infra the in vivo experiments).

By comparison of the data presented in Tables 2 and 3, it is quite clear that there is no correlation between the phenotypic integrin expression levels and efficacy of *cyclo*[DKP-RGD]-PTX conjugates in in vitro assays. The cell sensitivity studies were carried out to determine whether paclitaxel was released from the conjugate. In these in vitro assays, no tumor homing effect can be expected and therefore the different response can be attributed only to a higher or lower sensitivity of the different cell lines to the particular compound tested, independent of the integrin receptor expression. On the other hand, the evaluation of integrin expression was important for the choice of the best in vivo model for efficacy studies (i.e., the choice of cisplatin-resistant IGROV-1/Pt1, a cell line where the expression of integrin $\alpha_v\beta_3$ is particularly relevant).

Evaluation of in Vivo Antitumor Activity. Antitumor activity of our lead conjugate *cyclo*[DKP-*f*3-RGD]-PTX **11**, delivered intravenously (iv) and administered every 4 days for 4 times (q4d×4), was examined on the $\alpha_V\beta_3$-rich IGROV-1/Pt1 carcinoma grown in athymic mice as subcutaneous (sc) tumor. A significant, dose-related antitumor effect was observed following administration of two dose levels of compound **11** (15 and 30 mg/kg). Moreover, when compound **11** (30 mg/kg, i.e., 19.1 μmol/kg) was compared to paclitaxel (30 mg/kg, i.e., 35.1 μmol/kg) administered with the same weight dosage and schedule, it displayed better effects in terms of tumor volume inhibition (TVI, 85% vs 76%), despite the lower (about half) molar dosage used (Figure 8). Furthermore, 2 out of 8 tumors in animals receiving conjugate **11** disappeared without any evidence of disease until the end of the experiment. Thus, an improved and more persistent effect against the growth of treated tumors was achieved, as indicated also by the higher $\log_{10}$(cell kill) value (LCK of 1.4 vs 0.7, Table 4). Treatment was well tolerated, as no deaths or significant weight losses were observed among the treated animals.[36]

Immunohistochemistry Analysis of Treatment Effects. To investigate the mechanism underlying the improved antitumor activity of *cyclo*[DKP-*f*3-RGD]-PTX **11** over paclitaxel, histopathological analysis was carried out in tumors from untreated mice and from mice treated with *cyclo*[DKP-*f*3-RGD]-PTX **11**, compound **64**, and paclitaxel (Figure 9). The comparison between paclitaxel and *cyclo*[DKP-*f*3-RGD]-PTX **11** was carried out administering 30 mg/kg for both compounds, amounts that correspond to 35.1 μmol/kg for paclitaxel and to 19.1 μmol/kg for *cyclo*[DKP-*f*3-RGD]-PTX **11**. Histological analysis indicated the presence of a high

Table 2. Cell Sensitivity of Different Tumor Cell Lines to Compounds 10−13 and 64[a]

		IC_{50} (nM)					
compd	structure	IGROV-1	IGROV-1/Pt1	U2-OS	SKOV3	PANC-1	MIA-PaCa2
10	*cyclo*[DKP-*f*2-RGD]-PTX	17.7 ± 6.0	18.7 ± 6.0	2.2 ± 0.5	1.6 ± 1.0	5.8 ± 4.0	2.0 ± 0.7
11	*cyclo*[DKP-*f*3-RGD]-PTX	61.3 ± 19.1	4.9 ± 2.0	12.8 ± 0.1	1.2 ± 0.1	2.4 ± 0.8	2.3 ± 0.4
12	*cyclo*[DKP-*f*4-RGD]-PTX	34.4 ± 29.0	3.7 ± 2.0	6.8 ± 4.6	2.4 ± 0.9	3.2 ± 0.7	1.8 ± 0.6
13	*cyclo*[DKP-*f*6-RGD]-PTX	48.2 ± 2.2	2.4 ± 1.9	5.7 ± 4.4	2.4 ± 1.1	3.5 ± 0.1	2.5 ± 0.6
64	*cyclo*[DKP-*f*3-RGD]	>1200	>18000	>6300	>11600	>11600	>11600
PTX	paclitaxel	23.0 ± 0.8	2.2 ± 0.8	3.4 ± 0.4	2.7 ± 1.1	5.2 ± 1.9	7.2 ± 3.8

[a]Cell sensitivity was evaluated by growth inhibition assays based on cell counting. Cells were seeded, and 24 h later they were exposed to the compounds for 72 h. At the end of treatment, cells were counted using a cell counter.

dx.doi.org/10.1021/jm301058f | J. Med. Chem. XXXX, XXX, XXX−XXX

Table 3. Integrin Expression of Tumor Cell Lines of Different Tumor Types[a]

	mean fluorescence intensity					
integrin	IGROV-1	IGROV-1/Pt1	U2-OS	SKOV3	PANC-1	MIA-PaCa2
$\alpha_V\beta_3$	4.8 ± 1.9	23.3 ± 5.0	1.8 ± 0.6	6.4 ± 0.05	7.9 ± 2.8	1.2 ± 0.1
$\alpha_V\beta_5$	3.4 ± 0.9	3.3 ± 0.5	27.4 ± 0.1	4.4 ± 0.5	25.7 ± 6.5	5.6 ± 0.9

[a]Integrin expression levels were examined by immunofluorescence using a flow cytometer. The ratios between the mean fluorescence intensity of cells incubated with primary antibody and isotypic control are shown.

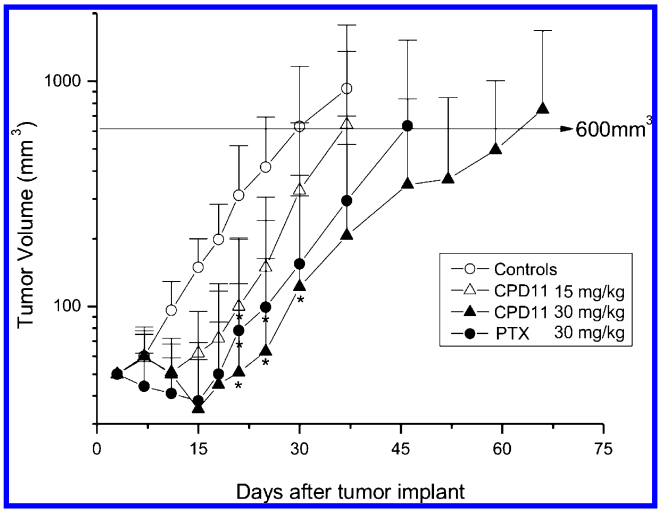

Figure 8. In vivo antitumor activity studies of *cyclo*[DKP-*f*3-RGD]-PTX **11** compared to paclitaxel on IGROV-1/Pt1 ovarian carcinoma. Shown is the efficacy of compound **11** (CPD11) and paclitaxel (PTX) administered intravenously every fourth day for four times on the ovarian carcinoma IGROV-1/Pt1 xenografted subcutaneously in athymic nude mice. The solvent was injected for the control group (○). Each point represents the mean tumor volume from eight tumors. Bars represent SD: ∗, $P < 0.05$ by Student's *t* test on tumor volumes over control mice.

number of mitotic cells in the group treated with *cyclo*[DKP-*f*3-RGD]-PTX **11**, compared to the other groups (Figure 9). In addition, the majority of the mitoses observed in the groups treated with either *cyclo*[DKP-*f*3-RGD]-PTX **11** or paclitaxel were aberrant, an observation consistent with the mechanism of action of spindle poisons.[37] High levels of aberrant mitoses were observed with *cyclo*[DKP-*f*3-RGD]-PTX **11**, already 24 h after the second treatment, and persisted after the fourth treatment. On the contrary, the amount of aberrant mitotic cells observed after mice treatment with paclitaxel decreased over time.

Since tumors from mice treated with *cyclo*[DKP-*f*3-RGD]-PTX **11** had the highest number of mitoses and the major part of them were atypical, it is likely that tumor cells treated with compound **11** entered mitosis but failed to replicate and incurred mitotic arrest.

CONCLUSIONS

Since α_V integrins are overexpressed on the surface of cancer cells, we have synthesized a small library of integrin ligand−paclitaxel conjugates **10**−**13** with the aim of using the tumor-homing *cyclo*[DKP-RGD] peptidomimetics for site-directed delivery of the cytotoxic drug. All the paclitaxel−RGD constructs **10**−**13** inhibited biotinylated vitronectin binding to the purified $\alpha_V\beta_3$ receptor at low nanomolar concentration, showing that the enormous increase of steric hindrance in the conjugates, due to presence of the linker bearing paclitaxel through the succinate tether, did not influence the high affinity for the integrin receptors. *cyclo*[DKP-RGD]-PTX conjugates **10**−**13** showed in vitro cytotoxic activity against a panel of human tumor cell lines similar to paclitaxel. Among the cell lines, the cisplatin-resistant IGROV-1/Pt1 cells expressed high levels of integrin $\alpha_V\beta_3$, making them attractive to be tested in in vivo models. *cyclo*[DKP-*f*3-RGD]-PTX **11** displayed sufficient stability in physiological solution and in both human and murine plasma to be a good candidate for in vivo testing. In tumor-targeting experiments against the IGROV-1/Pt1 human ovarian carcinoma xenotransplanted in nude mice, compound **11** exhibited better effects than paclitaxel in terms of tumor volume inhibition and $\log_{10}$(cell kill), despite the lower (about half) molar dosage used. Moreover, 2 out of 8 tumors in animals receiving conjugate **11** disappeared without any evidence of disease until the end of experiment, suggesting an improved and more persistent antitumor effect. Treatment was well tolerated, as no deaths or significant weight losses were observed among the treated animals. Results from comparison of the in vitro data shown in Table 2 (where conjugate **11** is apparently 2-fold less cytotoxic than paclitaxel with respect to the IGROV-1/Pt-1 cancer cell line) with the in vivo data of Table 4 and Figure 8 (where conjugate **11** shows a superior antitumor effect compared to paclitaxel against the IGROV-1/Pt1 human ovarian carcinoma xenotransplanted in nude mice) are not contradictory but rather reinforce the tumor homing effect claimed for compound **11**. In fact, in vivo the conjugate is targeted to the tumor, whereas in vitro it acts through release of paclitaxel. The histological examination of tumor specimens

Table 4. In Vivo Antitumor Activity and Toxicity Profile of *cyclo*[DKP-*f*3-RGD]-PTX 11 and Paclitaxel against Human Ovarian Cancer Xenografts (IGROV-1/Pt1) in Mice, as a Function of Dose

treatment	dose (mg/kg)	dose (μmol/kg)	TVI%[a]	CR[b]	NED[c]	LCK[d]	BWL%[e]	*D*/*T*[f]
paclitaxel	30	35.1	76	3/8	0/8	0.7	4	0/4
cyclo[DKP-*f*3-RGD]-PTX **11**	15	9.6	64	0/8		0.3	0	0/4
cyclo[DKP-*f*3-RGD]-PTX **11**	30	19.1	85	2/8	2/8	1.4	3	0/4

[a]TVI%: tumor volume inhibition percent in treated over control mice, calculated 10 days after the end of treatments. [b]CR: complete response, disappearance of tumors lasting at least 10 days. [c]NED: no evidence of disease at the end of experiment (at day 66). [d]LCK: gross $\log_{10}$(cell kill) to reach 600 mm^3 of tumor volume (see Figure 8). [e]BWL%: body weight loss percentage induced by drug treatment. [f]*D*/*T*: dead/treated mice.

dx.doi.org/10.1021/jm301058f | J. Med. Chem. XXXX, XXX, XXX−XXX

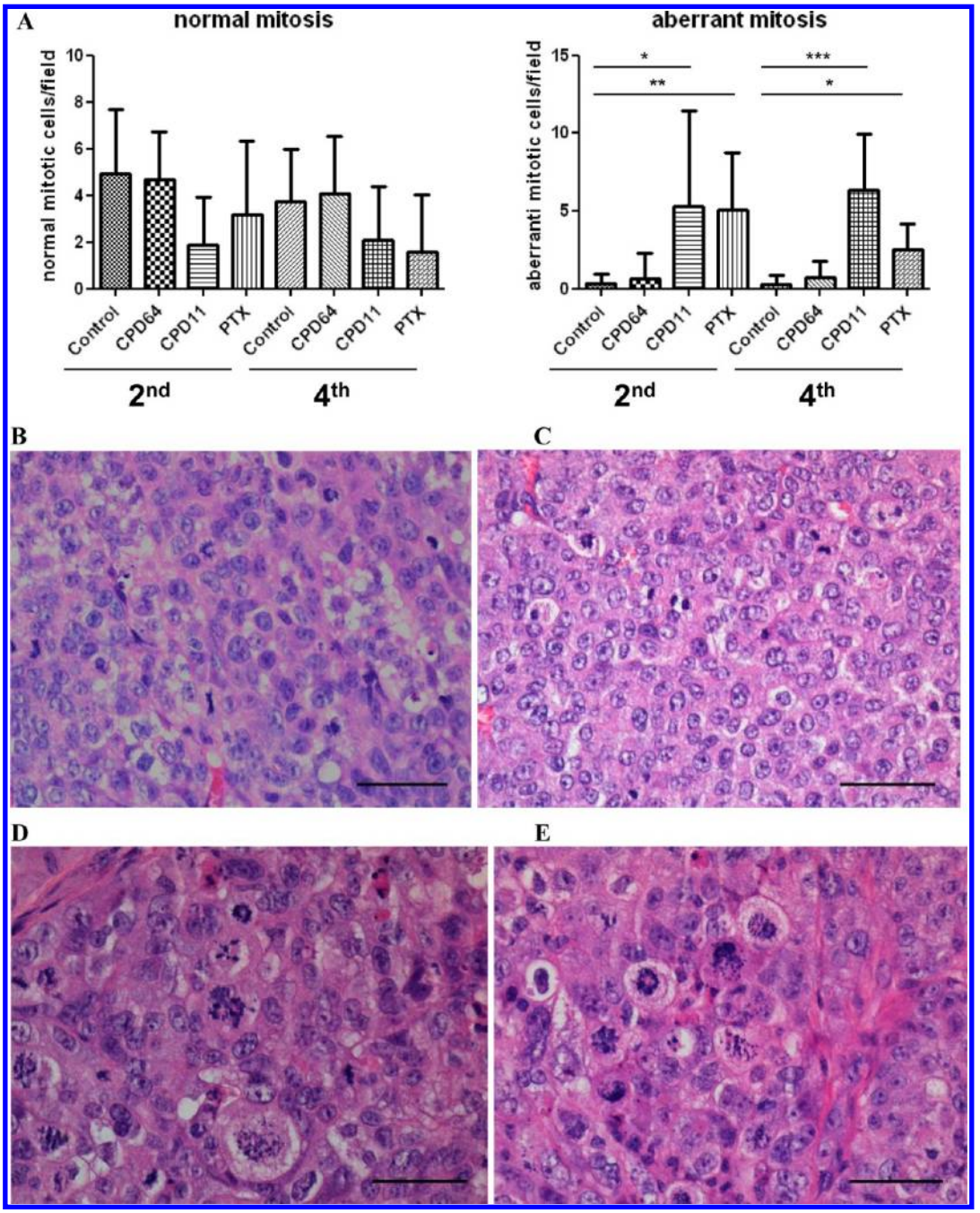

Figure 9. Histopathological analysis of IGROV-1/Pt1 xenograft after treatment with *cyclo*[DKP-*f*3-RGD]-PTX **11**. (A) Quantitative analysis of mitoses. Mitoses were evaluated in three randomly selected 400× fields using quadruplicate samples. The reported numbers correspond to the mean number of normal/aberrant mitoses in analyzed groups: control groups (control); groups treated with compound **64** (CPD64); group treated with compound **11** (CPD11); groups treated with paclitaxel (PTX). Note that tumors were obtained from mice sacrificed 24 h after the second or the fourth treatment. (B) Randomly selected high power field (hpf) within the bulk of the tumor from a control group sample, characterized by normal mitoses (hematoxylin and eosin; bar, 50 μm). (C) Randomly selected hpf within the bulk of the tumor from a sample treated with compound **64**. Hyperchromatic nuclei with condensed chromatin are evident (hematoxylin and eosin; bar, 50 μm). (D) Randomly selected hpf within the bulk of the tumor from a sample treated with compound **11**. Note markedly aberrant mitoses, with formation of nuclear envelopes around individual clusters of missegregated chromosomes (mitotic catastrophe) (hematoxylin and eosin; bar, 50 μm). (E) Randomly selected hpf within the bulk of the tumor from a sample treated with paclitaxel. Note markedly aberrant mitoses, with formation of nuclear envelopes around individual clusters of missegregated chromosomes (mitotic catastrophe) (hematoxylin and eosin; bar, 50 μm).

supports this view because the induction of aberrant mitosis observed after treatment with conjugate **11** was more frequent, pronounced, and persistent than that observed with paclitaxel (see Figure 9A, right diagram), consistent with a successful drug delivery to the target. The superior in vivo activity of *cyclo*[DKP-*f*3-RGD]-PTX **11** compared to paclitaxel supports the view that integrin ligands are promising tools to improve delivery of cytotoxic drugs.

EXPERIMENTAL SECTION

Materials and Methods. All manipulations requiring anhydrous conditions were carried out in flame-dried glassware, with magnetic

dx.doi.org/10.1021/jm301058f | J. Med. Chem. XXXX, XXX, XXX–XXX

stirring and under a nitrogen atmosphere. All commercially available reagents were used as received. Anhydrous solvents were purchased from commercial sources and withdrawn from the container by syringe under a slight positive pressure of nitrogen. (*S*)- and (*R*)-Serine methyl ester hydrochloride,[38] (2*R*)- and (2*S*)-aspartic acid β-allyl ester hydrochloride,[39] *N*-(*tert*-butoxycarbonyl)-(2*R*)-aspartic acid β-allyl ester,[39] (*S*)- and (*R*)-*N*-Boc-serine methyl ester,[40] (*S*)- and (*R*)-methyl 3-azido-2-(*tert*-butoxycarbonylamino)propanoate,[41] (*S*)- and (*R*)-3-azido-2-(*tert*-butoxycarbonylamino)propanoic acid,[41] (*S*)- and (*R*)-dimethyl aspartate hydrochloride,[42] (*S*)- and (*R*)-*N*-benzyldimethyl aspartate,[43] and *N*-Boc-glycine benzyl ester[44] were prepared according to literature procedures, and their analytical data were in agreement with those already published. Reactions were monitored by analytical thin layer chromatography using 0.25 mm precoated silica gel glass plates (DURASIL-25 UV254) and compounds visualized using UV fluorescence, aqueous potassium permanganate, or ninhydrin. Flash column chromatography was performed according to the method of Still and co-workers[45] using Chromagel 60 ACC (40−63 μm) silica gel. Melting points were obtained in an open capillary apparatus and are uncorrected. ^{1}H NMR spectra were recorded on a spectrometer operating at 400.16 MHz. Proton chemical shifts are reported in ppm (δ) with the solvent reference relative to tetramethylsilane (TMS) employed as the internal standard. The following abbreviations are used to describe spin multiplicity: s = singlet, d = doublet, t = triplet, q = quartet, m = multiplet, br = broad signal, dd = doublet of doublet. ^{13}C NMR spectra were recorded on a spectrometer operating at 100.63 MHz, with complete proton decoupling. Carbon chemical shifts are reported in ppm (δ) relative to TMS with the respective solvent resonance as the internal standard. Infrared spectra were recorded on a standard FT-IR, and peaks are reported in cm^{-1}. Optical rotation values were measured on an automatic polarimeter with a 1 dm cell at the sodium D line and are given in units of 10^{-1} deg cm^2 g^{-1}. High resolution mass spectrometry (HRMS) were performed on a Fourier transform ion cyclotron resonance (FT-ICR) mass spectrometer APEX II with Xmass software (Bruker Daltonics) and 4.7 T magnet (Magnex) equipped with ESI source, available at CIGA (Centro Interdipartimentale Grandi Apparecchiature) c/o Università degli Studi di Milano, Italy. Low resolution mass spectra were measured on a Waters Acquity UPLC−MS (ESI ion source). All described compounds showed a purity of >98%, as determined by HPLC (UV and MS detectors). LC−UV/MS data were collected with an Agilent 1100 HPLC instrument connected to a Bruker Esquire 3000+ ion trap mass spectrometer through an ES interface.

Cancer cell lines IGROV-1 and IGROV-1/Pt1 were obtained as previously reported.[46] Cancer cell lines U2OS, SKOV3, PANC-1, and MIA Paca2 are ATCC cultures, registered as follows: U2OS, ATCC HTB-96; SKOV3, ATCC HTB-77; PANC-1, ATCC CRL-1469; MIA PaCa2, ATCC CRL-1420.

Solid-Phase Receptor-Binding Assay. Purified $\alpha_v\beta_3$ and $\alpha_v\beta_5$ receptors (Chemicon International, Inc., Temecula, CA, U.S.) were diluted to 0.5 μg/mL in coating buffer containing 20 mM Tris-HCl (pH 7.4), 150 mM NaCl, 1 mM $MnCl_2$, 2 mM $CaCl_2$, and 1 mM $MgCl_2$. An aliquot of diluted receptors (100 μL/well) was added to 96-well microtiter plates (NUNC MW 96F MEDISORP STRAIGHT) and incubated overnight at 4 °C. The plates were then incubated with blocking solution (coating buffer plus 1% bovine serum albumin) for an additional 2 h at room temperature to block nonspecific binding followed by 3 h of incubation at room temperature with various concentrations (10^{-12}−10^{-5} M) of test compounds in the presence of 1 μg/mL biotinylated vitronectine. Biotinylation was performed using EZ-Link sulfo-NHS-biotinylation kit (Pierce, Rockford, IL). After being washed, the plates were incubated for 1 h at room temperature with streptavidin−biotinylated peroxidase complex (Amersham Biosciences, Uppsala, Sweden) followed by 30 min of incubation with 100 μL of substrate reagent solution (R&D Systems, Minneapolis, MN) before the reaction was stopped by addition of 50 μL of 2 N H_2SO_4. Absorbance at 415 nm was read in a Synergy HT multidetection microplate reader (BioTek Instruments, Inc.). Each data point is the result of the average of triplicate wells and was analyzed by nonlinear regression analysis with the Prism GraphPad program.

General Procedure A for Deprotection Reactions. To a solution of the *N*-Boc-protected amino acid or peptide in CH_2Cl_2 (0.13 M) was added half volume of TFA, and the mixture was stirred at room temperature for 2 h. The solvent was evaporated, toluene (2×) was added followed by evaporation, and then ether was added and evaporated to afford the corresponding TFA salt.

General Procedure B for Coupling Reactions. To a solution of the *N*-protected amino acid in DMF under nitrogen atmosphere and at 0 °C were added HATU (1.2 equiv), HOAt (1.2 equiv), and *i*-Pr_2NEt (4 equiv). After 30 min, a solution of the TFA salt of the peptide in DMF was added, and the reaction mixture was stirred at 0 °C for 1 h and at room temperature overnight. The mixture was diluted with AcOEt and consecutively washed with 1 M $KHSO_4$ (2×), aqueous $NaHCO_3$ (2×), and brine (2×), dried over Na_2SO_4 and the solvent evaporated under reduced pressure to afford the crude product.

General Procedure C for the Synthesis of *cyclo*[DKP-RGD]−Paclitaxel Conjugates 10−13. Diisopropylcarbodiimide (11.93 μL, 9.72 mg, 0.077 mmol, 1.9 equiv) was added to a solution of 2′-succinylpaclitaxel **67** (49 mg, 0.0513 mmol, 1.25 equiv) and *N*-hydroxysulfosuccinimide sodium salt (13.94 mg, 0.0642 mmol, 1.55 equiv) in dry dimethylformamide (2.0 mL). The resulting solution was stirred under argon at room temperature for 24 h. Volatiles were then removed in vacuo to give an off-white solid, which was redissolved in acetonitrile (2 mL). A solution of the appropriate *cyclo*[DKP-RGD] (**63−66**) (35 mg, 0.0414 mmol) in pH 7.0 phosphate buffer (0.5 M, 1.0 mL) was then added to the acetonitrile solution, and the pH was adjusted to 7.3 with NaOH (0.2 M, a few drops). The resulting solution was rapidly cooled to 0 °C and stirred for 10 h, warmed to room temperature, and stirred for further 18 h. During the entire period the pH was kept near 7.3, adding 0.1 M aqueous NaOH when required. Dioxane/water (1:1, 10 mL) was then added to the reaction mixture, and the resulting solution was freeze-dried. The solid recovered from freeze-drying was purified by semipreparative HPLC [Water's Atlantis 21 mm × 10 cm column, gradient of 90% (H_2O + 0.1% HCOOH)/10% (CH_3CN + 0.1% HCOOH) to 30% (H_2O + 0.1% HCOOH)/70% (CH_3CN + 0.1% HCOOH)]. The purified products were then freeze-dried to give the desired compounds (**10−13**) as white solids.

***cyclo*[DKP-*f*2-RGD]-PTX 10.** Compound **10** was synthesized according to general procedure C (40 mg, 60% yield). ^{1}H NMR (400 MHz, CD_3OD) δ 8.09 (dd, 2H, *J* = 8.4, 1.2 Hz), 7.84 (dd, 2H, *J* = 7.1, 1.6 Hz), 7.74 (tt, 1H, *J* = 6.8, 1.6 Hz), 7.64 (t, 2H, *J* = 7.6 Hz), 7.59−7.54 (m, 1H), 7.49−7.44 (m, 6H), 7.28−7.25 (m, 4H), 7.22 (tt, 1H, *J* = 5.8, 2.8 Hz), 6.43 (s, 1H), 5.98 (t, 1H, *J* = 9.1 Hz), 5.69 (d, 1H, *J* = 7.9 Hz), 5.61 (d, 1H, *J* = 7.0 Hz), 5.45 (d, 1H, *J* = 7.9 Hz), 5.24 (d, 1H, *J* = 15.1 Hz), 5.10 (dd, 1H, *J* = 9.7, 1.6 Hz), 4.77 (m overlapped with water signal, 1H), 4.65 (m overlapped with water signal, 1H), 4.40−4.30 (m, 4H), 4.21 (m, 3H), 4.08 (d, 2H, *J* = 15.7 Hz), 3.85 (d, 1H, *J* = 4.6 Hz), 3.78 (d, 1H, *J* = 7.0 Hz), 3.64 (d, 1H, *J* = 16.3 Hz), 3.28 (m overlapped with solvent signal, 1H), 3.22 (t, 2H, *J* = 6.7 Hz), 2.98 (dd, 1H, *J* = 13.2, 7.4 Hz), 2.84−2.75 (m, 2H), 2.71−2.68 (m, 2H), 2.64−2.50 (m, 3H), 2.37−2.34 (m, 4H), 2.18 (s, 3H), 2.01 (m, 1H), 1.89−1.79 (m, 5H), 1.75−1.59 (m, 7H), 1.14 (s, 3H), 1.11 (s, 3H); ^{13}C NMR (101 MHz, CD_3OD) δ 205.7, 175.8, 175.0, 174.5, 174.17, 174.02, 173.7, 172.09, 171.96, 171.1, 170.74, 170.54, 169.8, 168.0, 158.3, 142.3, 139.6, 137.9, 135.5, 135.04, 134.95, 134.7, 133.2, 131.1, 130.8, 130.2, 129.94, 129.82, 129.71, 129.3, 129.0, 128.64, 128.46, 85.9, 82.0, 79.1, 77.5, 76.7, 76.14, 76.06, 72.9, 72.1, 60.3, 59.1, 55.8, 55.4, 53.2, 51.3, 48.1, 47.8, 44.3, 43.7, 43.0, 40.7, 39.9, 37.32, 37.21, 36.0, 31.0, 29.9, 28.2, 26.8, 26.2, 23.4, 22.3, 20.9, 15.0, 10.6; IR (film) 3361, 3075, 2940, 1730, 1715, 1698, 1667, 1538, 1422, 1243, 1135, 1072 cm^{-1}. MS (ESI) *m*/*z* calcd for $[C_{78}H_{92}N_{11}O_{24}]^+$, 1566.63 $[M + H]^+$; found, 1566.6.

***cyclo*[DKP-*f*3-RGD]-PTX 11.** Compound **11** was synthesized according to general procedure C (47 mg, 70% yield). ^{1}H NMR (400 MHz, CD_3OD) δ 8.12 (dd, 2H, *J* = 8.5, 1.4 Hz), 7.83 (dd, 2H, *J* = 8.5, 1.4 Hz), 7.71−7.66 (m, 1H), 7.60 (t, 2H, *J* = 7.5 Hz), 7.56−7.52

dx.doi.org/10.1021/jm301058f | J. Med. Chem. XXXX, XXX, XXX−XXX

(m, 1H), 7.50−7.42 (m, 6H), 7.30 (s, 4H), 7.25 (tt, 1H, J = 7.1, 1.6 Hz), 6.45 (s, 1H), 6.05 (td, 1H, J = 9.1, 1.0 Hz), 5.79 (d, 1H, J = 6.5 Hz), 5.64 (d, 1H, J = 7.2 Hz), 5.44 (d, 1H, J = 6.5 Hz), 5.13 (d, 1H, J = 14.9 Hz), 5.03 (dd, 1H, J = 9.4, 1.6 Hz), 4.91−3.86 (m, 1H), 4.75 (dd, 1H, J = 6.5, 4.7 Hz), 4.44−4.36 (m, 3H), 4.30−4.22 (m, 2H), 4.20 (br s, 2H, J = 4.2 Hz), 4.16 (ddd, 1H, J = 12.0, 8.7, 3.6 Hz), 4.09−4.08 (m, 2H), 3.90 (d, 1H, J = 6.0 Hz), 3.82 (d, 1H, J = 7.1 Hz), 3.74−3.68 (m, 2H), 3.61 (d, 1H, J = 17.2 Hz), 3.54 (dt, 1H, J = 11.7, 2.8 Hz), 3.42 (dd, 1H, J = 14.6, 6.4), 3.27−3.16 (m, 2H), 2.80−2.75 (m, 2H), 2.72−2.51 (m, 7H), 2.37 (s, 3H), 2.18−2.12 (m, 4H), 2.09−2.01 (m, 1H), 1.92 (s, 3H), 1.86−1.76 (m, 3H), 1.68−1.63 (m, 5H), 1.14 (s, 3H), 1.13 (s, 3H); ^{13}C NMR (101 MHz, CD_3OD) δ 205.5, 174.0, 173.60, 173.46, 173.0, 171.63, 171.54, 171.46, 171.2, 170.5, 167.7, 142.4, 140.2, 138.4, 135.5, 134.80, 134.63, 132.9, 131.39, 131.22, 130.1, 129.72, 129.60, 129.56, 129.3, 128.6, 100.0, 85.9, 82.3, 79.0, 77.5, 76.9, 76.2, 75.9, 72.9, 72.4, 61.6, 60.6, 59.2, 55.4, 54.4, 53.2, 50.5, 48.0, 44.6, 43.76, 43.69, 42.2, 39.9, 37.6, 36.49, 36.36, 31.1, 29.8, 27.7, 26.9, 26.5, 25.1, 23.3, 22.3, 20.8, 15.1, 10.5; IR (film) 3360, 3075, 2940, 1729, 1714, 1693, 1665, 1537, 1421, 1241, 1135, 1071 cm^{-1}. MS (ESI) m/z calcd for $[C_{78}H_{92}N_{11}O_{24}]^+$, 1566.63 $[M + H]^+$; found, 1566.6.

***cyclo*[DKP-*f*4-RGD]-PTX 12.** Compound **12** was synthesized according to general procedure C (42 mg, 63% yield). ^{1}H NMR (400 MHz, DMSO-d_6) δ 9.22 (d, 1H, J = 8.5 Hz), 8.95 (s, 1H), 8.79 (s, 1H), 8.44−8.40 (m, 1H), 8.35 (t, 1H, J = 5.7 Hz), 8.20 (s, 1H), 7.98 (dd, 2H, J = 7.1, 1.3 Hz), 7.86 (dd, 2H, J = 7.2, 1.3 Hz), 7.76−7.69 (m, 1H, J = 1.5 Hz), 7.69−7.63 (m, 2H), 7.59−7.53 (m, 1H), 7.49 (d, 1H, J = 7.6 Hz), 7.46−7.42 (m, 5H), 7.23−7.17 (m, 5H), 6.30 (s, 1H), 5.83 (t, 1H, J = 8.9 Hz), 5.54 (t, 1H, J = 8.7 Hz), 5.42 (d, 1H, J = 7.1 Hz), 5.36 (d, 1H, J = 8.9 Hz), 5.21 (d, 1H, J = 14.4 Hz), 4.92 (d, 2H, J = 10.6 Hz), 4.62 (s, 1H), 4.27−4.07 (m, 5H), 4.04−3.99 (m, 3H), 3.94−3.87 (m, 1H), 3.83−3.79 (m, 1H), 3.70 (br s, 2H), 3.58 (d, 1H, J = 7.1 Hz), 3.43−3.26 (m overlapped with water signal, 2H), 3.07 (br s, 2H), 2.89 (br s, 2H), 2.69−2.56 (m, 3H), 2.45 (t, 2H, J = 6.8 Hz), 2.38−2.30 (m, 2H), 2.24−2.20 (m, 4H), 2.10 (s, 3H), 1.84−1.76 (m, 5H), 1.64 (t, 1H, J = 12.4 Hz), 1.54−1.41 (m, 7H), 1.02 (s, 3H), 1.00 (s, 3H); ^{13}C NMR (101 MHz, DMSO-d_6) δ 202.3, 173.9, 172.13, 171.94, 170.8, 170.2, 169.63, 169.50, 169.1, 168.84, 168.74, 168.3, 167.9, 166.4, 165.2, 157.3, 139.4, 138.7, 137.3, 134.8, 134.3, 133.45, 133.33, 132.7, 131.4, 129.95, 129.93, 129.56, 129.54, 128.73, 128.65, 128.55, 128.29, 128.14, 127.83, 127.71, 127.65, 127.4, 83.6, 80.2, 76.7, 75.3, 74.68, 74.54, 74.50, 72.5, 70.7, 70.4, 57.4, 56.1, 53.98, 53.86, 52.17, 52.13, 46.1, 44.9, 42.9, 42.1, 41.9, 40.1, 39.9, 38.2, 36.5, 35.7, 34.4, 29.5, 28.7, 27.6, 26.3, 25.3, 22.5, 21.4, 20.63, 20.52, 13.9, 9.7; IR (film) 3370, 3071, 2941, 1731, 1714, 1699, 1667, 1538, 1421, 1243, 1135, 1071 cm^{-1}, MS (ESI) m/z calcd for $[C_{78}H_{92}N_{11}O_{24}]^+$, 1566.63 $[M + H]^+$; found, 1566.6.

***cyclo*[DKP-*f*6-RGD]-PTX 13.** Compound **13** was synthesized according to general procedure C (43 mg, 65% yield). ^{1}H NMR (400 MHz, DMSO-d_6) δ 9.42 (s, 1H), 9.25 (d, 1H, J = 8.5 Hz), 8.74 (s, 1H), 8.62 (s, 1H), 8.45 (s, 1H), 8.37 (t, 1H, J = 5.7 Hz), 7.99−7.97 (m, 2H), 7.87−7.84 (m, 3H), 7.73 (t, 1H, J = 7.3 Hz), 7.66 (t, 2H, J = 7.4 Hz), 7.56 (tt, 1H, J = 7.3, 2.0 Hz), 7.50−7.44 (m, 7H), 7.25−7.15 (m, 5H), 6.30 (s, 1H), 5.83 (t, 1H, J = 8.8 Hz), 5.53 (t, 1H, J = 8.7 Hz), 5.41 (d, 1H, J = 7.2 Hz), 5.35 (d, 1H, J = 9.0 Hz), 5.11 (d, 1H, J = 14.9 Hz), 4.98−4.90 (t, 2H), 4.64 (s, 1H), 4.29−4.20 (m, 3H), 4.17−4.08 (m, 2H), 4.04−3.95 (m, 3H), 3.93−3.79 (m, 3H), 3.74−3.64 (m, 1H), 3.59 (d, 1H, J = 6.8 Hz), 3.53−3.43 (m, 1H), 3.26−3.19 (m, 1H), 3.07 (br s, 1H), 2.97 (br s, 1H), 2.72−2.58 (m, 4H), 2.56−2.52 (m, 1H), 2.45 (t, 2H, J = 6.8 Hz), 2.40−2.28 (m, 2H), 2.23 (s, 3H), 2.10 (s, 3H), 1.82−1.60 (m, 7H), 1.52−1.46 (m, 6H), 1.02 (s, 3H), 1.00 (s, 3H); ^{13}C NMR (101 MHz, DMSO-d_6) δ 202.7, 172.0, 171.8, 170.3, 169.72, 169.57, 169.2, 168.79, 168.72, 166.8, 166.4, 165.2, 157.3, 139.5, 137.4, 135.2, 134.3, 133.5, 133.32, 133.28, 132.7, 131.5, 129.9, 129.6, 128.7, 128.38, 128.21, 128.0, 127.7, 127.5, 83.6, 80.3, 76.7, 75.3, 74.69, 74.62, 74.49, 70.7, 70.4, 57.2, 54.4, 54.1, 51.98, 51.92, 46.10, 45.97, 43.0, 41.9, 40.9, 39.7, 37.8, 36.6, 34.4, 29.5, 28.7, 28.0, 26.4, 24.4, 22.6, 21.4, 20.7, 14.0, 9.8; IR (film) 3365, 3071, 2940, 1732, 1716, 1699, 1665, 1537, 1421, 1243, 1135, 1071 cm^{-1}. MS (ESI) m/z calcd for $[C_{78}H_{92}N_{11}O_{24}]^+$, 1566.63 $[M + H]^+$; found, 1566.6.

Plasma Stability Assays. A 10 mM stock solution of *cyclo*[DKP-*f*3-RGD]-PTX **11** (MW = 1566.62) was obtained by dissolving 2 mg of compound in 127.66 μL of DMSO. A further dilution 1:50 in pH 7.5 phosphate buffer (PBS) was performed (10 μL of stock solution into 490 μL of PBS) to obtain a 200 μM solution. From this last solution, an amount of 25 μL was spiked into 475 μL of plasma (murine or human) to obtain the final concentration of 10 μM. Standards (lidocaine and 2-piperidinoethyl-4-amino-5-chloro-2-methoxybenzoate) were tested at 2.5 μM final concentration starting from a 500 μM stock solution in DMSO, further diluted 1:10 into PBS and 1:20 into plasma.

Aliquots of 50 μL volume were taken at 0, 15, 30, 60, 120, 180, and 300 min of incubation at 37 °C and immediately quenched with 200 μL of a solution of verapamil, 250 ng/mL (internal standard) in acetonitrile. Samples were centrifuged for 20 min at 3000 rpm and supernatants analyzed by UPLC (Waters) interfaced with a Premiere XE triple quadrupole (Waters). Eluents were the following: phase A, 95% H_2O, 5% CH_3CN + 0.1% HCOOH; phase B, 5% H_2O, 95% CH_3CN + 0.1% HCOOH. Waters UPLC parameters were the following: flow of 0.6 mL/min, column BEH C18, 50 mm × 2.1 mm, 1.7 μm, at 50 °C, vol injection of 5 μL. Samples were analyzed in multiple reaction monitoring (MRM) conditions: ESI positive, desolvation temperature 450 °C, desolvation gas 900 L/h, cone gas 90 L/h, collision gas 0.2 L/h. Results are presented as the mean ± SD, n = 2 for standards, n = 3 for *cyclo*[DKP-*f*3-RGD]-PTX **11**.

Cell Sensitivity Studies. The human ovarian carcinoma IGROV-1 cell line,[46] the cisplatin-resistant IGROV-1/Pt1 subline,[46] the human ovarian carcinoma cell line SKOV3, and the human pancreatic carcinoma cell lines PANC-1 and MIA-PaCa2 were cultured in Dulbecco's modified Eagle medium (DMEM) medium. The human osteosarcoma U2-OS cell line was grown in McCoy's 5A medium. HDFC cells were cultured in DMEM-F12 medium. In all cases, the medium was supplemented with 10% fetal calf serum. The cell sensitivity to drugs was measured by using the growth inhibition assay based on cell counting. Cells were seeded in duplicate into six-well plates and exposed to drug 24 h later. Paclitaxel and the studied compounds were dissolved in DMSO and then added to culture medium. DMSO concentration in medium never exceeded 0.25%. After 72 h of drug incubation, cells were harvested for counting with a cell counter (Z1 Beckman Coulter counter). IC_{50} is defined as the drug concentration producing 50% decrease of cell growth. At least five independent experiments were performed.

Analysis of Integrin Levels. The expression of integrins was measured by flow cytometry, following optimization of antibody concentration. Exponentially growing cells were harvested and incubated for 30 min at 4 °C with anti-human $\alpha_v\beta_3$ or $\alpha_v\beta_5$ antibodies or isotypic controls (Millipore, Temecula, CA; Chemicon International). Cells were than washed, and samples were immediately used for flow cytometric analysis (FACScan, Becton-Dickinson). Expression of integrins was expressed as the ratio between the mean fluorescence intensity obtained in cells incubated with anti-integrin antibodies divided by that of cells incubated with isotypic control.

In Vivo Antitumor Activity Studies. All experiments were carried out using female athymic Swiss nude mice, 8−10 weeks old (Charles River, Calco, Italy). Mice were maintained in laminar flow rooms, keeping temperature and humidity constant. Mice had free access to food and water. Experiments were approved by the Ethics Committee for Animal Experimentation of the Istituto Nazionale Tumori of Milan, Italy, according to institutional guidelines. The IGROV-1/Pt1 human tumor xenograft, derived from cultures of the corresponding ovarian carcinoma cell line,[46] was used. Exponentially growing cells (10^7/mouse) were sc injected into the right flank of athymic nude mice, and the tumor line was achieved by serial sc passages of fragments of regrowing tumors into healthy mice. Groups of four mice bearing bilateral sc tumors were employed. Tumor fragments were implanted on day 0, and tumor growth was followed by biweekly measurements of tumor diameters with a Vernier caliper. Tumor volume (TV) was calculated according to the formula TV (mm^3) = $d^2D/2$, where d and D are the shortest and the longest diameter, respectively. Compounds were delivered iv and administered

dx.doi.org/10.1021/jm301058f | J. Med. Chem. XXXX, XXX, XXX−XXX

every 4 days for 4 times (q4d×4). Treatment started 3 days after tumor implant, when tumors were just palpable. The efficacy of the drug treatment was assessed as (1) tumor volume inhibition percentage (TVI%) in treated versus control mice, calculated as TVI % = [100 − (mean TV treated/mean TV control)] × 100), (2) $\log_{10}$(cell kill) (LCK) calculated by the formula LCK = $(T - C)/(3.32\ DT)$ where T and C are the mean times (days) required for treated and control tumors, respectively, to reach an established TV, and DT is the doubling time of control tumors, obtained from semilog best-fit curves of mean tumor volumes plotted against time, and (3) complete regression (CR), i.e., disappearance of the tumor lasting at least 10 days after the end of treatments. Tumors not regrown at the end of experiment were considered as no evidence of disease (NED). The toxicity of the drug treatment was determined as body weight loss (BWL) and lethal toxicity (D/T, dead/treated mice). The highest body weight loss percentage induced by treatments is reported in the tables. Deaths occurring in treated mice before the death of the first control mouse were ascribed to toxic effects. Two-sided Student's t test was used for statistical comparison of tumor volumes in control over treated mice. For in vivo studies, paclitaxel was dissolved in a mixture of ethanol and Cremophor ELP (50% + 50%) and kept at 4 °C. At treatment the drug was diluted in 90% of cold saline after magnetic stirring and administered iv. *cyclo*[DKP-*f*3-RGD]-PTX **11** was dissolved and administered like paclitaxel at room temperature.

Immunohistochemistry. Tumor xenografts and adjacent tissues were excised and formalin-fixed and paraffin-embedded. Sections of 4 μm from each tumor xenograft were routinely stained with hematoxylin−eosin (HE) and evaluated under a light microscope. Mitoses were evaluated in three randomly selected 400× fields within the bulk of the xenograft, avoiding areas of necrosis and hemorrhage. The total number of mitoses and the mean value for each sample were evaluated. Furthermore, mitoses were classified as "normal" and "aberrant", considering in this latter class both small condensed hyperchromatic nuclei and large cells composed by nuclear envelope around individual clusters of missegregated chromosomes (mitotic catastrophe), and the ratio between these two classes was evaluated. The analysis of mitoses was performed in a blind fashion. Statistical analysis of the obtained data was carried out with Kruskal−Wallis test followed by Dunn's multiple comparison test using GraphPad Prism (GraphPad Software, Inc.).

■ ASSOCIATED CONTENT

Supporting Information

General information for syntheses and biological procedures, detailed experimental procedures for the synthesis of compounds **10**−**68**, and ^{1}H and ^{13}C NMR for all new compounds. This material is available free of charge via the Internet at http://pubs.acs.org.

■ AUTHOR INFORMATION

Corresponding Author

*For U.P.: phone, +39-031-2386444; fax, +39-031-2386449; e-mail, umberto.piarulli@uninsubria.it. For C.G.: phone, +39-02-50314091; fax, +39-02-50314072; e-mail, cesare.gennari@unimi.it.

Notes

The authors declare no competing financial interest.

■ ACKNOWLEDGMENTS

We thank Milan University, Italy, for Ph.D. fellowships (to M.M. and R.C.) and Indena S.p.A. for a generous gift of paclitaxel. We also gratefully acknowledge Ministero dell'Università e della Ricerca for financial support (PRIN Project: Synthesis and Biomedical Applications of Tumor-Targeting Peptidomimetics). U.P. thanks Fondazione CARIPLO for a research grant (Project: RedDrug-Train).

■ ABBREVIATIONS USED

DKP, diketopiperazine; Mtr, 4-methoxy-2,3,6-trimethylbenzenesulfonamide; HATU, *O*-(7-azabenzotriazol-1-yl)-*N*,*N*,*N*′,*N*′-tetramethyluronium hexafluorophosphate; Tol, toluene; TEA, triethylamine; HOAT, 1-hydroxy-7-azabenzotriazole; DIAD, diisopropyl azodicarboxylate; BOC-ON, 2-(Boc-oxyimino)-2-phenylacetonitrile; DCU, *N*,*N*′-dicyclohexylurea; PyBrOP, bromotripyrrolidinophosphonium hexafluorophosphate; DPPA, diphenylphosphorylazide; EDT, 1,2-ethanedithiol; TIPS, triisopropylsilane; DIC, *N*,*N*′-diisopropylcarbodiimide; sulfo-NHS, *N*-hydroxysulfosuccinimide sodium salt; PTX, paclitaxel; RP-HPLC, reverse phase high-pressure liquid chromatography; HDFC, human dermal fibroblast cell; TVI, tumor volume inhibition; CR, complete response; NED, no evidence of disease; LCK, $\log_{10}$(cell kill); BWL, body weight loss; D/T, dead/treated mice; MRM, multiple reaction monitoring; DMEM, Dulbecco's modified Eagle medium; TV, tumor volume

■ REFERENCES

(1) Broxterman, H. J.; Lankelma, J.; Hoekman, K. Resistance to cytotoxic and anti-angiogenic anticancer agents: similarities and differences. *Drug Resist. Updates* **2003**, *6*, 111−127.

(2) Siepmann, J.; Siegel, R. A.; Rathbone, M. J. *Fundamentals and Applications of Controlled Release Drug Delivery*; Springer: New York, 2012; pp 493−516.

(3) (a) Lammers, T.; Kiessling, F.; Hennink, W. E.; Storm, G. Drug targeting to tumors: principles, pitfalls and (pre-) clinical progress. *J. Controlled Release* **2012**, *161*, 175−187. (b) Kratz, F.; Müller, I. A.; Ryppa, C.; Warnecke, A. Prodrug strategies in anticancer chemotherapy. *ChemMedChem* **2008**, *3*, 20−53.

(4) (a) Low, P. S. The optimal strategy for drug targeting. *Mol. Pharmacol.* **2007**, *4*, 629−630. (b) Aina, O. H.; Liu, R. W.; Sutcliffe, J. L.; Marik, J.; Pan, C. X.; Lam, K. S. From combinatorial chemistry to cancer-targeting peptides. *Mol. Pharmacol.* **2007**, *4*, 631−651.

(5) (a) Ruoslahti, E.; Bhatia, S. N.; Sailor, M. J. Targeting of drugs and nanoparticles to tumors. *J. Cell Biol.* **2010**, *188*, 759−768. (b) Mahato, R.; Tai, W.; Cheng, K. Prodrugs for improving tumor targetability and efficiency. *Adv. Drug Delivery Rev.* **2011**, *63*, 659−670.

(6) Lu, X.; Lu, D.; Scully, M.; Kakkar, V. The role of integrins in cancer and the development of anti-integrin therapeutic agents for cancer therapy. *Perspect. Med. Chem.* **2008**, *2*, 57−73.

(7) Barczyk, M.; Carracedo, S.; Gullberg, D. Integrins. *Cell Tissue Res.* **2010**, *339*, 269−280.

(8) Hynes, R. O. Integrins: bidirectional, allosteric signaling machines. *Cell* **2002**, *110*, 673−687.

(9) (a) Shimaoka, M.; Springer, T. A. Therapeutic antagonists and conformational regulation of integrin function. *Nat. Rev. Drug Discovery* **2003**, *2*, 703−716. (b) Rathinam, R.; Alahari, S. K. Important role of integrins in the cancer biology. *Cancer Metastasis Rev.* **2010**, *29*, 223−237.

(10) Plow, E. F.; Haas, T. A.; Zhang, L.; Loftus, J.; Smith, J. W. Ligand binding to integrins. *J. Biol. Chem.* **2000**, *275*, 21785−21788.

(11) Dechantsreiter, M. A.; Planker, E.; Mathä, B.; Lohof, E.; Hölzemann, G.; Jonczyk, A.; Goodman, S. L.; Kessler, H. N-Methylated cyclic RGD peptides as highly active and selective $\alpha_v\beta_3$ integrin antagonists. *J. Med. Chem.* **1999**, *42*, 3033−3040.

(12) Gottschalk, K. E.; Kessler, H. The structures of integrins and integrin−ligand complexes: implications for drug design and signal transduction. *Angew. Chem., Int. Ed.* **2002**, *41*, 3967−3774.

(13) Mas-Moruno, C.; Rechenmacher, F.; Kessler, H. Cilengitide: the first anti-angiogenic small molecule drug candidate design, synthesis and clinical evaluation. *Anti-Cancer Agents Med. Chem.* **2010**, *10*, 753−768.

(14) Xiong, J.-P.; Stehle, T.; Zhang, R.; Joachimiak, A.; Frech, M.; Goodman, S. L.; Arnaout, M. A. Crystal structure of the extracellular

segment of integrin $\alpha_V\beta_3$ in complex with an Arg-Gly-Asp ligand. *Science* **2002**, *296*, 151−155.
(15) Auzzas, L.; Zanardi, F.; Battistini, L.; Burreddu, P.; Carta, P.; Rassu, G.; Curti, C.; Casiraghi, G. Targeting $\alpha_V\beta_3$ integrin: design and applications of mono- and multifunctional RGD-based peptides and semipeptides. *Curr. Med. Chem.* **2010**, *17*, 1255−1299.
(16) (a) Ressurreicao, A. S. M.; Vidu, A.; Civera, M.; Belvisi, L.; Potenza, D.; Manzoni, L.; Ongeri, S.; Gennari, C.; Piarulli, U. Cyclic RGD-peptidomimetics containing bifunctional diketopiperazine scaffolds as new potent integrin ligands. *Chem.—Eur. J.* **2009**, *15*, 12184−12188. (b) Marchini, M.; Mingozzi, M.; Colombo, R.; Guzzetti, I.; Belvisi, L.; Vasile, F.; Potenza, D.; Piarulli, U.; Arosio, D.; Gennari, C. Cyclic RGD-peptidomimetics containing bifunctional diketopiperazine scaffolds as new potent integrin ligands. *Chem.—Eur. J.* **2012**, *18*, 6195−6207.
(17) (a) Reynolds, A. R.; Hart, I. R.; Watson, A. R.; Welti, J. C.; Silva, R. G.; Robinson, S. D.; Da Violante, G.; Gourlaouen, M.; Salih, M.; Jones, M. C.; Jones, D. T.; Saunders, G.; Kostourou, V.; Perron-Sierra, F.; Norman, J. C.; Tucker, G. C.; Hodivala-Dilke, K. M. Stimulation of tumor growth and angiogenesis by low concentrations of RGD-mimetic integrin inhibitors. *Nat. Med.* **2009**, *15*, 392−400. (b) Weis, S. M.; Stupack, D. G.; Cheresh, D. A. Agonizing integrin antagonists? *Cancer Cell* **2009**, *15*, 359−361. (c) Shabbir, S. H.; Eisenberg, J. L.; Mrksich, M. An inhibitor of a cell adhesion receptor stimulates cell migration. *Angew. Chem., Int. Ed.* **2010**, *49*, 7706−7709. (d) Robinson, S. D.; Hodivala-Dilke, K. M. The role of β3-integrins in tumor angiogenesis: context is everything. *Curr. Opin. Cell Biol.* **2011**, *23*, 630−637.
(18) Chen, K.; Chen, X. Integrin targeted delivery of chemotherapeutics. *Theranostics* **2011**, *1*, 189−200.
(19) (a) Arap, W.; Pasqualini, R.; Ruoslahti, E. Cancer treatment by targeted drug delivery to tumor vasculature in a mouse model. *Science* **1998**, *279*, 377−80. (b) Kim, J. W.; Lee, H. S. Tumor targeting by doxorubicin-RGD-4C peptide conjugate in an orthotopic mouse hepatoma model. *Int. J. Mol. Med.* **2004**, *14*, 529−535.
(20) Burkhart, D. J.; Kalet, B. T.; Coleman, M. P.; Post, G. C.; Koch, T. H. Doxorubicin−formaldehyde conjugates targeting $\alpha v\beta$3 integrin. *Mol. Cancer Ther.* **2004**, *3*, 1593−604.
(21) Ryppa, C.; Mann-Steinberg, H.; Fichtner, I.; Weber, H.; Satchi-Fainaro, R.; Biniossek, M. L.; Kratz, F. In vitro and in vivo evaluation of doxorubicin conjugates with the divalent peptide E-[c(RGDfK)$_2$] that targets integrin $\alpha_v\beta_3$. *Bioconjugate Chem.* **2008**, *19*, 1414−22.
(22) Mukhopadhyay, S.; Barnés, C. M.; Haskel, A.; Short, S. M.; Barnes, K. R.; Lippard, S. J. Conjugated platinum(IV)-peptide complexes for targeting angiogenic tumor vasculature. *Bioconjugate Chem.* **2008**, *19*, 39−49.
(23) (a) Dal Pozzo, A.; Ni, M. H.; Esposito, E.; Dallavalle, S.; Musso, L.; Bargiotti, A.; Pisano, C.; Vesci, L.; Bucci, F.; Castorina, M.; Fodera, R.; Giannini, G.; Aulicino, C.; Penco, S. Novel tumor-targeted RGD peptide-camptothecin conjugates: synthesis and biological evaluation. *Bioorg. Med. Chem. Lett.* **2010**, *18*, 64−72. (b) Alloatti, D.; Giannini, G.; Vesci, L.; Castorina, M.; Pisano, C.; Badaloni, E.; Cabri, W. Camptothecins in tumor homing via an RGD sequence mimetic. *Bioorg. Med. Chem. Lett.* **2012**, *22*, 6509−6512.
(24) (a) Chen, X.; Plasencia, C.; Hou, Y.; Neamati, N. Synthesis and biological evaluation of dimeric RGD peptide-paclitaxel conjugate as a model for integrin-targeted drug delivery. *J. Med. Chem.* **2005**, *48*, 1098−106 (corrigendum *J. Med. Chem.* **2005**, *48*, 5874). (b) Cao, Q.; Li, Z.-B.; Chen, K.; Wu, Z.; He, L.; Neamati, N.; Chen, X. Evaluation of biodistribution and anti-tumor effect of a dimeric RGD peptide-paclitaxel conjugate in mice with breast cancer. *Eur. J. Nucl. Med. Mol. Imaging* **2008**, *35*, 1489−98.
(25) Ryppa, C.; Mann-Steinberg, H.; Biniossek, M. L.; Satchi-Fainaro, R.; Kratz, F. In vitro and in vivo evaluation of a paclitaxel conjugate with the divalent peptide E-[c(RGDfK)$_2$] that targets integrin $\alpha_V\beta_3$. *Int. J. Pharm.* **2009**, *368*, 89−97.
(26) Marchini, M.; Mingozzi, M.; Colombo, R.; Gennari, C.; Durini, M.; Piarulli, U. Selective *O*-acylation of unprotected *N*-benzylserine methyl ester and *O*,*N*-acyl transfer in the formation of cyclo[Asp-Ser] diketopiperazines. *Tetrahedron* **2010**, *66*, 9528−9531.
(27) Choi, H.; Aldrich, J. V. Comparison of methods for the Fmoc solid-phase synthesis and cleavage of a peptide containing both tryptophan and arginine. *Int. J. Pept. Protein Res.* **1993**, *42*, 58−63.
(28) Deutsch, H. M.; Glinski, J. A.; Hernandez, M.; Haugwitz, R. D.; Narayanan, V. L.; Suffness, M.; Zalkow, L. H. Synthesis of congeners and prodrugs. 3. Water-soluble prodrugs of Taxol with potent antitumor activity. *J. Med. Chem.* **1989**, *32*, 788−792.
(29) (a) Buchegger, F.; Kosinski, M.; Viertl, D.; Poitry-Yamate, C.; Baechler, S.; Prior, J. Tumor localization and mouse-derived dosimetry projection for Ga-68-NODAGA-RGD PET. *J. Nucl. Med. Meet. Abstr.* **2011**, *52*, 1487. (b) Ye, Y.; Zhu, L.; Ma, Y.; Niu, G.; Chen, X. Synthesis and evaluation of new iRGD peptide analogs for tumor optical imaging. *Bioorg. Med. Chem. Lett.* **2011**, *21*, 1146−1150.
(30) Liu, S.; Liu, Z.; Chen, K.; Yan, Y.; Watzlowik, P.; Wester, H. J.; Chin, F. T.; Chen, X. ^{18}F-Labeled galacto and PEGylated RGD dimers for PET imaging of $\alpha_v\beta_3$ integrin expression. *Mol. Imaging Biol.* **2010**, *12*, 530−538.
(31) (a) Fani, M.; Psimadas, D.; Zikos, C.; Xanthopoulos, S.; Loudos, G. K.; Bouziotis, P.; Varvarigou, A. D. Comparative evaluation of linear and cyclic ^{99m}Tc-RGD peptides for targeting of integrins in tumor angiogenesis. *Anticancer Res.* **2006**, *26*, 431−434. (b) Lang, L.; Li, W.; Guo, N.; Ma, Y.; Kiesewetter, D. O.; Niu, G.; Chen, X. Comparison study of [^{18}F]FAl-NOTA-PRGD2, [^{18}F]FPPRGD2, and [^{68}Ga]Ga-NOTA-PRGD2 for PET imaging of U87MG tumors in mice. *Bioconjugate Chem.* **2011**, *22*, 2415−2422. (c) Li, W.; Lang, L.; Niu, G.; Guo, N.; Ma, Y.; Kiesewetter, D. O.; Shen, B.; Chen, X. *N*-Succinimidyl 4-[^{18}F]-fluoromethylbenzoate-labeled dimeric RGD peptide for imaging tumor integrin expression. *Amino Acids* **2012**, *43*, 1349−1357.
(32) (a) Janssen, M. L.; Oyen, W. J.; Dijkgraaf, I.; Massuger, L. F.; Frielink, C.; Edwards, D. S.; Rajopadhye, M.; Boonstra, H.; Corstens, F. H.; Boerman, O. C. Tumor targeting with radiolabeled $\alpha_v\beta_3$ integrin binding peptides in a nude mouse model. *Cancer Res.* **2002**, *62*, 6146−6151. (b) Lanzardo, S.; Conti, L.; Brioschi, C.; Bartolomeo, M. P.; Arosio, D.; Belvisi, L.; Manzoni, L.; Maiocchi, A.; Maisano, F.; Forni, G. A new optical imaging probe targeting $\alpha_v\beta_3$ integrin in glioblastoma xenografts. *Contrast Media Mol. Imaging* **2011**, *6*, 449−458.
(33) Haubner, R.; Schmitt, W.; Hö1lzemann, G.; Goodman, S. L.; Jonczyk, A.; Kessler, H. Cyclic RGD peptides containing β-turn mimetics. *J. Am. Chem. Soc.* **1996**, *118*, 7881−7891.
(34) Manzoni, L.; Belvisi, L.; Arosio, D.; Civera, M.; Pilkington-Miksa, M.; Potenza, D.; Caprini, A.; Araldi, E. M. V.; Monferrini, E.; Mancino, M.; Podestà, F.; Scolastico, C. Cyclic RGD-including functionalized azabicycloalkane amino acids as potent integrin antagonists for tumor targeting. *ChemMedChem* **2009**, *4*, 615−632 and references cited therein..
(35) Fu, Y.; Li, S.; Zu, Y.; Yang, G.; Yang, Z.; Luo, M.; Jiang, S.; Wink, M.; Efferth, T. Medicinal chemistry of paclitaxel and its analogues. *Curr. Med. Chem.* **2009**, *16*, 3966−3985.
(36) Recently, a azabicycloalkane-RGD bound to paclitaxel via a cleavable diglycolyl ester linker at C2′ was reported to provide promising in vitro and in vivo antitumor activity. See the following: Pilkington-Miksa, M.; Arosio, D.; Battistini, L.; Belvisi, L.; De Matteo, M.; Vasile, F.; Burreddu, P.; Carta, P.; Rassu, G.; Perego, P.; Carenini, N.; Zunino, F.; De Cesare, M.; Castiglioni, V.; Scanziani, E.; Scolastico, C.; Casiraghi, C.; Zanardi, F.; Manzoni, L. Design, synthesis and biological evaluation of novel cRGD-paclitaxel conjugates for integrin-assisted drug delivery. *Bioconjugate Chem.* **2012**, *23*, 1610−1622.
(37) (a) Matson, D. R.; Stukenberg, P. T. Spindle poisons and cell fate: a tale of two pathways. *Mol. Interventions* **2011**, *11*, 141−150. (b) Portugal, J.; Mandilla, S.; Bataller, M. Mechanisms of drug-induced mitotic catastrophe in cancer cells. *Curr. Pharm. Des.* **2010**, *16*, 69−78. (c) Roninson, I. B.; Broude, E. V.; Chang, B. D. If not apoptosis, then what? Treatment-induced senescence and mitotic catastrophe in tumor cells. *Drug Resist. Updates* **2001**, *4*, 303−313.

(38) Huang, Y.; Dalton, D. R.; Carroll, P. J. The efficient, enantioselective synthesis of aza sugars from amino acids. 1. The polyhydroxylated pyrrolidines. *J. Org. Chem.* **1997**, *62*, 372−376.
(39) Webster, K. L.; Maude, A. B.; O'Donnell, M. E.; Mehrotra, A. P.; Gani, D. Design and preparation of serine−threonine protein phosphatase inhibitors based upon the nodularin and microcystin toxin structures. Part 3. *J. Chem. Soc., Perkin Trans. 1* **2001**, 1673−1695.
(40) Pirrung, M. C.; Shuey, S. W. Photoremovable protecting groups for phosphorylation of chiral alcohols. Asymmetric synthesis of phosphotriesters of (−)-3′,5′-dimethoxybenzoin. *J. Org. Chem.* **1994**, *59*, 3890−3897.
(41) Rosenberg, S. H.; Spina, K. P.; Woods, K. W.; Polakowski, J.; Martin, D. L.; Yao, Z.; Stein, H. H.; Cohen, J.; Barlow, J. L.; Egan, D. A.; Tricarico, K. A.; Baker, W. R.; Kleinert, H. D. Studies directed toward the design of orally active renin inhibitors. 1. Some factors influencing the absorption of small peptides. *J. Med. Chem.* **1993**, *36*, 449−459.
(42) Gu, K.; Bi, L.; Zhao, M.; Wang, C.; Ju, J.; Peng, S. Toward the development of chemoprevention agents. Part 1: Design, synthesis, and anti-inflammatory activities of a new class of 2,5-disubstituted-dioxacycloalkanes. *Bioorg. Med. Chem.* **2007**, *15*, 6273−6290.
(43) Humphrey, J. M.; Bridges, R. J.; Hart, J. A.; Chamberlin, A. R. 2,3-Pyrrolidinedicarboxylates as neurotransmitter conformer mimics: enantioselective synthesis via chelation-controlled enolate alkylation. *J. Org. Chem.* **1994**, *59*, 2467−2472.
(44) Narukawa, Y.; Juneau, K. N.; Snustad, D.; Miller, D. B.; Hegedus, L. S. Synthesis of optically active β-lactams by the photolytic reaction of imines with optically active chromium carbene complexes. 2. Synthesis of 1-carbacephalothin and 3-ANA relays. *J. Org. Chem.* **1992**, *57*, 5453−5462.
(45) Still, W. C.; Kahn, M.; Mitra, A. Rapid chromatographic techniques for preparative separation with moderate resolution. *J. Org. Chem.* **1978**, *43*, 2923−2925.
(46) (a) Perego, P.; Romanelli, S.; Carenini, N.; Magnani, I.; Leone, R.; Bonetti, A.; Paolicchi, A.; Zunino, F. Ovarian cancer cisplatin-resistant cell lines: multiple changes including collateral sensitivity to Taxol. *Ann. Oncol.* **1998**, *9*, 1−8. (b) Perego, P.; Giarola, M.; Righetti, S. C.; Supino, R.; Caserini, C.; Delia, D.; Pierotti, M. A.; Miyashita, T.; Reed, J. C.; Zunino, F. Association between cisplatin resistance and mutation of p53 gene and reduced bax expression in ovarian carcinoma cell systems. *Cancer Res.* **1996**, *56*, 556−562.